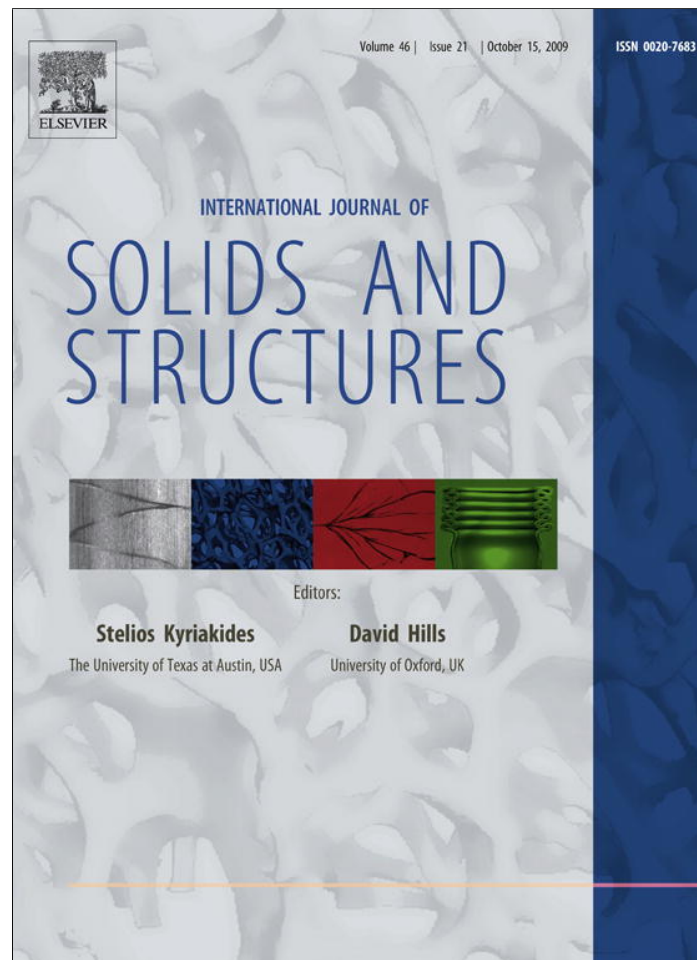


Provided for non-commercial research and education use.
Not for reproduction, distribution or commercial use.



This article appeared in a journal published by Elsevier. The attached copy is furnished to the author for internal non-commercial research and education use, including for instruction at the authors institution and sharing with colleagues.

Other uses, including reproduction and distribution, or selling or licensing copies, or posting to personal, institutional or third party websites are prohibited.

In most cases authors are permitted to post their version of the article (e.g. in Word or Tex form) to their personal website or institutional repository. Authors requiring further information regarding Elsevier's archiving and manuscript policies are encouraged to visit:

<http://www.elsevier.com/copyright>



Contents lists available at ScienceDirect

International Journal of Solids and Structures

journal homepage: www.elsevier.com/locate/ijsolstr

Quantum field induced strains in nanostructures and prospects for optical actuation

Xinyuan Zhang^a, Mohamed Gharbi^a, Pradeep Sharma^{a,b,*}, Harley T. Johnson^c^a Department of Mechanical Engineering, University of Houston, Houston, TX 77204, USA^b Department of Physics, University of Houston, Houston, TX 77204, USA^c Department of Mechanical Science and Engineering, University of Illinois at Urbana-Champaign, Urbana, IL 61801, USA

ARTICLE INFO

Article history:

Received 5 January 2009

Received in revised form 24 June 2009

Available online 22 July 2009

Keywords:

Quantum dots

Strain

Electronic structure

Polaron

ABSTRACT

We develop the mechanics theory of a phenomenon in which strain is induced in nanoscale structures in the absence of applied stress, due solely to the presence of quantum mechanical confinement of charge carriers. The direct effect of strain on electronic structure has been widely studied in recent years, but the “reverse coupling” effect that we investigate, which is only appreciable in the smallest structures, has been largely ignored even though its effects are present in first principles atomistic calculations. We develop a simple effective mass approach that can be used to model this universal physical phenomenon allowing a transparent scheme to identify its occurrence. We relate quantum field induced strain to acoustic polarons and identify the presence of this effect in density functional theory calculations of strain and quantum confinement in free-standing Si and GaAs quantum dots. Finally, we discuss the use of this quantum confinement induced strain as a mechanism for universal optical actuation in nano-wire structures in the context of recent experimental results on carbon nanotubes.

© 2009 Elsevier Ltd. All rights reserved.

1. Introduction and background

In the mechanics of solids, thermal coupling to strain is well known. Even in the complete absence of mechanical forces, a change in temperature induces mechanical strain. If part of the solid subjected to the thermal field is mechanically constrained, internal stresses may also arise. There are other similar possible physical couplings. In certain materials, electrical or magnetic fields may also induce strain – these effects, unlike thermoelastic coupling, are not universal (at least not if one restricts consideration to the linearized “small field” assumption). In the present article we explore a somewhat unusual type of physical coupling: *mechanical strain due to changes in quantum field*. We demonstrate that this coupling is strongly size-dependent and occurs only in nanostructures. We use quantum dots as a model system to investigate this fundamental effect.

In three-dimensional structures with dimensions on the scale of nanometers, often referred to as quantum dots (QDs), quantum mechanical effects that would be negligible in macroscopic structures become significant. For example, electron energy spectra become discrete, with measurable energy differences between individual levels. Spectra are characterized by sharp densities of states reminiscent of atoms, and charge carriers are confined in all three spatial dimensions. These structures often consist of

* Corresponding author. Address: Department of Mechanical Engineering, University of Houston, Houston, TX 77204, USA. Tel.: +1 281 723 4649.

E-mail address: psharma@uh.edu (P. Sharma).

semiconductor material, and can be free standing, attached to a substrate or embedded in another material. Quantum dots are useful in revealing interesting basic science, and are also important for many emerging technological applications, such as next generation lighting (Arakawa, 2002; Nakamura et al., 2002), lasers (Bhattacharya, 2000; Deppe and Huffaker, 2000), quantum computing, information storage and quantum cryptography (Chye et al., 2002; Lundstrom et al., 1999; Petroff, 2003), biological labels (Alivisatos, 2000), sensors (Bhattacharya et al., 2002) and many others (Bandhyopadhyay and Nalwa, 2003; Bimberg, 1999; Bimberg et al., 1996; Grundmann et al., 1995; Tersoff et al., 1996; Williamson and Zunger, 1998).

Using standard top-down or bottom-up semiconductor fabrication approaches, quantum dots are often grown on lattice mismatched substrates, or embedded in lattice mismatched matrix materials, resulting in large elastic strains. Many groups have studied the effects of this strain on the electronic structure of quantum dots, which governs other transport and spectral properties fundamental in many device applications (Bimberg et al., 1996; Davies, 2000; Singh, 1992; Yu and Cardona, 2004). As shown in Fig. 1, elastic strain modifies the basic band structure parameters in semiconductor material. Dilatational strain modifies the band gap; axial and shear components of strain break the crystalline symmetry which lifts the energy degeneracy of the heavy hole and light hole valence subbands. This coupling between strain and electronic structure, particularly in quantum dots where elastic fields are highly nonuniform, has been widely studied, and is relevant for many emerging applications (e.g. Jiang and Singh, 1997; Johnson et al., 1998; Stier et al., 1999). In particular, the reader is referred

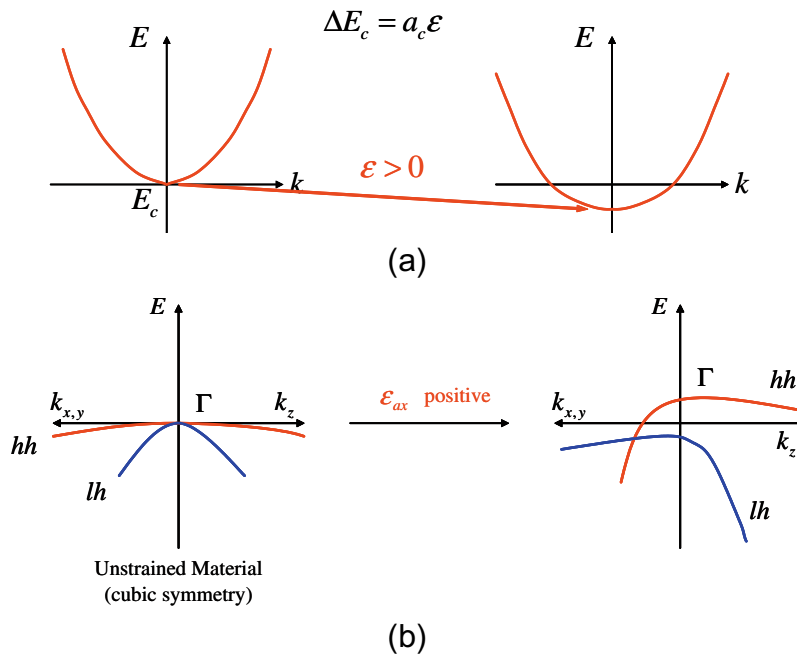


Fig. 1. (a) Effect of strain on the conduction band, or ΔE_c , due to dilatational strain. (b) Effect of strain on the valence band. Symmetry is broken by an axial component of strain. The terms “hh” and “lh” denote heavy hole and light hole band, respectively. ε denotes strain, k is the wave number and a_c is the deformation potential constant. Adapted from Davies (2000).

to a review article on this subject (Maranganti and Sharma, 2006) and two papers that appear in this journal (Freund and Johnson, 2001; Johnson and Bose, 2003).

In this work we report on the mechanisms of the “reverse effect”, i.e. inducing mechanical strain through changes in the quantum confinement, or more generally the electronic structure, even in the absence of an externally applied stress.

The outline of the paper is as follows: First, to illustrate this phenomenon in the simplest possible terms and to provide an intuitive physical understanding, we construct an elementary effective medium continuum model of quantum confinement induced strain in Section 2 and describe how this so-called reverse coupling may be interpreted in terms of quasiparticles called polarons (which are electron-frozen phonon pairs). A more sophisticated multi-band envelope function approach to the problem is constructed in Section 3 and numerical results are presented for Si and GaAs quantum dots in Section 4. Band edge shifts, induced strain field due to polarons and polaron binding energy are calculated. In Section 5, we illustrate the prospects of utilizing this effect to provide a universal mechanism for optical actuation of small nanowires. To verify our model and to obtain additional physical insights, we also perform, for smaller size quantum dots, ab initio calculations based on parameter-free self-consistent density functional theory (DFT) in both local density and generalized gradient approximations for the polaron binding energy. Larger quantum dots beyond the computational capability of DFT are handled via semi-empirical atomistic methods. The conventional envelope function method (EFM), unlike our modified EFM model or atomistic calculations, predicts zero polaron binding energy for all QD sizes. The present work is partially based on our previous article (Zhang et al., 2007) that discusses the same subject from a condensed matter viewpoint.

2. Single band toy model of quantum confinement induced strain and physical interpretation

In this section, inspired by the particle-in-a-box model widely presented in textbooks, we develop a similar model to illustrate

the phenomenon of quantum confinement induced strain. We consider a charge carrier, such as an electron, in a quantum dot. This model is less accurate in the case of the smallest quantum dots but the intent in this section is to highlight the general ideas. We assume that a known strain field exists that interacts with the electronic structure and perturbs it. Within the assumptions of the single band toy model under consideration, the impact of the strain on the electronic structure may be computed by solving the following equations (Davies, 2000):

$$\left(E_c - \frac{\hbar^2}{2m^*} \nabla^2 \right) \psi(\mathbf{r}) + a_c \cdot \text{Tr}(\varepsilon) \psi(\mathbf{r}) = E \psi(\mathbf{r})$$

$$\varepsilon = \varepsilon^0; \quad \sigma = \mathbf{C} : \varepsilon; \quad \text{div} \sigma = \mathbf{0} \quad (1)$$

Here m^* is the effective mass of the electron, σ and ε are elastic stress and strain tensor, respectively, and are constrained to obey the linearized elasticity relation $\sigma = \mathbf{C} : \varepsilon$. The Cauchy strain is the symmetric part of displacement gradient, i.e. $\varepsilon = \frac{1}{2}(\nabla \mathbf{u} + \nabla^T \mathbf{u})$. E_c is the energy of the band edge for the conduction or valence band.¹ a_c is the so-called deformation potential constant and determines the extent to which mechanical strain modifies the electronic structure of the quantum dot, e.g. its band gap.

We note that Eq. (1) allows only for a *one-way coupling*; i.e. strain can modify the electronic structure and hence the band gap and a host of opto-electronic properties of quantum dots but not vice versa; *changes in electronic structure* do not modify the strain. In the following we show that Eq. (1) are only approximate in this sense.

The total Lagrangian of the coupled system (the charge carrier and the continuum), apart from the unperturbed cohesive energy, is the summation of contributions from the carrier, the elastic field and the interactions between them (Emin and Holstein, 1976), or

¹ If dealing with the valence band, identical equations apply but the effective mass and the deformation potential constants are different, than in the conduction band case.

$$L_{\text{tot}}(u, \nabla u, \psi, \nabla \psi) = L_E + L_e + L_{\text{interaction}} \quad (2)$$

where,

$$\begin{aligned} L_E &= \int_V \left[-\frac{1}{2} \boldsymbol{\sigma} : \boldsymbol{\varepsilon} \right] d\mathbf{x} \\ L_e &= \int_V \left\{ \psi^\dagger E_c \psi - \frac{\hbar^2}{2m^*} \nabla \psi^\dagger \cdot \nabla \psi \right\} d\mathbf{x} \\ L_{\text{interaction}} &= \int_V \psi^\dagger (-a_c \text{Tr}(\boldsymbol{\varepsilon})) \psi d\mathbf{x} \\ \boldsymbol{\varepsilon} &= \frac{1}{2} (\nabla \mathbf{u} + \nabla^T \mathbf{u}) \end{aligned} \quad (3)$$

Using standard variational techniques (e.g. the Euler-Lagrange equations), and assuming elastic isotropy we obtain the following governing equations:

$$\begin{aligned} \left(E_c - \frac{\hbar^2}{2m^*} \nabla^2 \right) \psi(\mathbf{r}) + a_c \cdot \text{Tr}(\boldsymbol{\varepsilon}) \psi(\mathbf{r}) &= E \psi(\mathbf{r}) \\ \boldsymbol{\varepsilon} = \boldsymbol{\varepsilon}^0 - \underbrace{\frac{a_c}{3K} |\psi(\mathbf{r})|^2 \mathbf{I}} + \frac{3K(1-2\nu)}{(1+\nu)} \boldsymbol{\varepsilon} + \frac{3K\nu}{1+\nu} \text{Tr}(\boldsymbol{\varepsilon}) \mathbf{I}; \quad \text{div} \boldsymbol{\sigma} &= \mathbf{0} \end{aligned} \quad (4)$$

Here, K is the bulk modulus of the quantum dot, ν is the Poisson's ratio and E is the electronic spectrum of energies. We note now that changes in the quantum field (via the wave function) can also modify the strain field in the form of a “reverse coupling”. As already evident from Eq. (1), the typical practice is to ignore the bracketed term in Eq. (4). An interesting corollary to Eq. (4) is that even in complete absence of external strain, i.e. $\boldsymbol{\varepsilon}^0 = 0$, a dilatational strain proportional to the probability density $|\psi(\mathbf{r})|^2$ emerges. The square of the wavefunction scales inversely with size and thus we expect this “quantum confinement induced strain” to be appreciable only for very small sizes. This simple result is the basis of our paper. Small changes in the confinement or the quantum field via changes in the size, or electrical fields or any other mechanisms will induce a mechanical strain applied in quantum dots of sufficiently small size. Choosing Si as an example, the induced strain is estimated to be around 0.024% for a ~ 3 nm cubic quantum dot (with the choice of as 6.4 eV) and K as 98 GPa (Paul, 2004; Peng et al., 2006) – not a negligible insubstantial amount by the standards of continuum mechanics.

In position space $|\psi(\mathbf{r})|^2$ represents the spatial probability density distribution of the charge carrier. The strain field is proportional to the charge density and thus implies that the charge carrier moves along with an associated displacement. The electron coupling to a “deformation cloud”, in a discrete view, is referred to as polaron (Emin, 1972; Emin and Holstein, 1976) – and thus is a type of electron-frozen acoustic phonon pair. A polaron is depicted conceptually in Fig. 2.

Thus, a polaron caused by electron–phonon coupling, in our context, is a charge carrier that carries with it a localized lattice deformation field. Any field that disturbs the electron (e.g. increased or decreased confinement, applied electric fields, etc.) will also disturb the distortion field surrounding it, thus modifying the strain implied by Eq. (4). Thus, changes in the electronic motion can cause changes in the attached distortion around the charge carrier.

The *acoustic polaron* corresponds to an interaction between the carrier and the acoustic phonons, which, in a long wavelength approximation, form the elastic strain field. Therefore, the interaction between the carrier and the strain field, through Eqs. (2)–(4), correspond to the *formation of acoustic polarons*. The latter are quite different from piezoelectric and optical polarons, which are discussed widely in the condensed matter literature (Mahan, 2000). The piezoelectric polaron is related to the carrier–piezoelectric

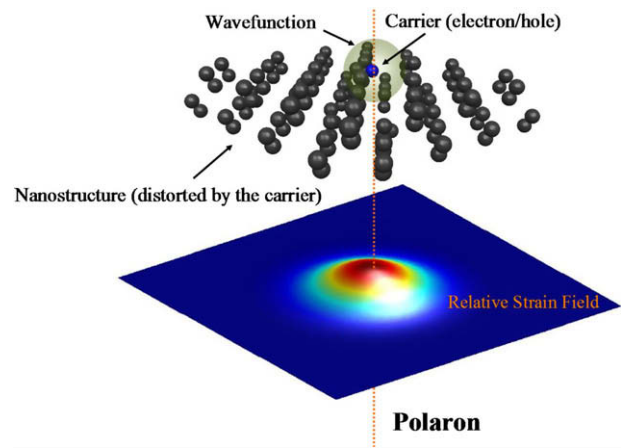


Fig. 2. Pictorial representation of an acoustic polaron. A charge carrier carries along with a local distortion. Perturbation of the charge carrier (which interacts with quantum fields) changes the distortion surrounding the charge carrier (i.e. perturbs the polaron) manifesting as an observable mechanical strain.

phonon interaction. The optical polaron (Bastard et al., 2002; Minnaert, 2001), or polar coupling polaron, is caused by the interaction of electrons and optical phonons. Optical polarons are mostly important for polar materials, including most II–VI or III–V semiconductors. The latter have already been investigated for quantum dots through an all-discrete approach (Bastard et al., 2002; Minnaert, 2001). In the present work, only the acoustic polarons (which are relevant to the elastic–quantum field coupling) will be investigated, although we will provide more perspective on this when we compare results for Si quantum dots (non-polar) with CdSe (polar).

We note here that the strictly dilatational nature of the quantum confinement induced strain is due to the assumed isotropy of the elastic properties and the nature of the single band toy model. This artifact is removed when we construct a more rigorous model in the next section.

3. General theory and multiband envelope function method

There are numerous atomistic electronic structure calculation methods, ranging from computationally expensive first principles atomistic methods in the category of density functional theory (DFT) approaches, to semi-empirical methods such as the empirical pseudopotential method (EPM) and the tight-binding approach (TB). Continuum or effective medium approaches such as the envelope function method (EFM) offer significant computational advantages, but are limited in accuracy which restrict their use to certain classes of problems. Nevertheless, for many systems these methods are the only practical approaches. Several recent reviews compare various electronic structure methods and the continuum approaches in particular (Bastard, 1991; Davies, 2000; Singh, 1992; Yu and Cardona, 2004).

The EFM approach in the 8×8 Hamiltonian form (Kane, 1966) is an effective medium approach that accounts for three spin-degenerate valence energy subbands and one spin-degenerate conduction energy subband in the bulk electronic structure. The unknown envelope part of the wave function is tensor-valued over the 8 subband basis, and the effective mass, a material property, is tensor-valued over the spatial coordinates. Finding the envelope part of the wave function requires the numerical solution of a steady state Schrödinger equation for the electron and hole energy eigenvalues in this tensor-valued framework. This model has been frequently applied to quantum dots (Efros and Rosen, 1998; Gashimzade et al., 2000; Pryor, 1998; Sercel et al., 1999; Sercel

and Vahala, 1990; Stier et al., 1999) and even to quantum dot heterostructures (see for example, Burt, 1992, 1999). This approach increases in accuracy if more than 4 energy bands are retained in the basis set – indeed, the well known particle-in-a-box toy problem (discussed in the previous section) corresponds to a single band approximation in one spatial dimension, whereby the tensor unknowns reduce to scalars. Mechanical strain can be accounted for in the Kane model as a perturbation of the 8×8 standard Hamiltonian (e.g. Bastard, 1991; Davies, 2000; Pollak, 1990; Singh, 1992; Stier et al., 1999; Yu and Cardona, 2004), albeit one that is readily tractable numerically. In this formalism, non-homogeneous strains may also be dealt with rigorously via the work of Zhang (1994).

In this approach the strain itself is usually calculated *a priori* by means of continuum elasticity (numerically or analytically depending on geometrical and anisotropic assumptions) and sometimes through empirical force field molecular dynamics (e.g. Andreev et al., 1999; Bellaiche et al., 1996; Bernard and Zunger, 1994; Cusack et al., 1996; Davies, 2000; Davies et al., 2002; Downes et al., 1997; Ellaway and Faux, 2002; Glas, 2001; Grundmann et al., 1995; Jiang and Singh, 1997; Johnson and Freund, 2001; Johnson et al., 1998; Keating, 1966; Korkusinski and Hawrylak, 2001; Makeev and Madhukar, 2003; Martin, 1970; Migliorato et al., 2002; Nishi et al., 1994; Pan and Yang, 2001; Pearson and Faux, 2000; Pryor, 1998; Pryor et al., 1998; Pryor et al., 1997; Romanov et al., 2001; Shin et al., 2003; Stillinger and Weber, 1985; Tadic et al., 2002; Yang et al., 1997; Yu and Madhukar, 1997a,b). The envelope function approach is attractive, simple and physically intuitive and thus widely used for both bulk semiconductors and nanostructures. However, this standard approach suffers from several shortcomings and its applicability to nanostructures appears questionable. Indeed, several authors have discussed this (see, for example the review by Carlo (2003)) and alternative atomistic approaches such as the TB method, EPM or DFT are often preferable when dealing with small quantum dots in the size-range of a few nanometers. In various works Zunger and co-workers (1996, 1999, 2001) have highlighted and clarified the various shortcomings of the envelope function approach when compared with EPM calculations. Wang and Zunger (1996, 1999) have made an important advance by modifying the standard envelope function approach to be more accurate for small quantum dots. While the EPM is fairly accurate provided the pseudopotential that replaces the effect of the core electrons and the nucleus has been well fitted empirically, it is computationally expensive for large systems, underscoring the importance of the Wang–Zunger works (1996, 1999) on the modification of the $\mathbf{k}\cdot\mathbf{p}$ model for quantum dots. Self-consistent DFT computations, while parameter free, often tend to underestimate the energies as DFT is best suited for only ground state energy calculations. Even within DFT, accuracy may suffer if the typically used local density approximation is used in place of more accurately modeling nonlocal effects. Nevertheless, relative effects are often faithfully captured by DFT and its advantage of being parameter-free is notable for new materials and effects. Applications are, however, generally limited to quantum dots smaller than 2.5 nm in diameter and indeed embedded quantum dots often prove to be beyond computational reach. More discussion on the applicability of DFT to the problem addressed in this paper is provided in Section 5.

In this section we develop a modified EFM approach that incorporates the “reverse coupling” illustrated earlier using the single band toy model. While quantum confinement induced strain is always implicitly present in numerical calculations, the toy model in the preceding section and the more sophisticated approach developed here allows us to separate this effect.

Based on a discrete model of polarons, an EFM model may be constructed following Emin and Holstein (1976). Alternatively, in

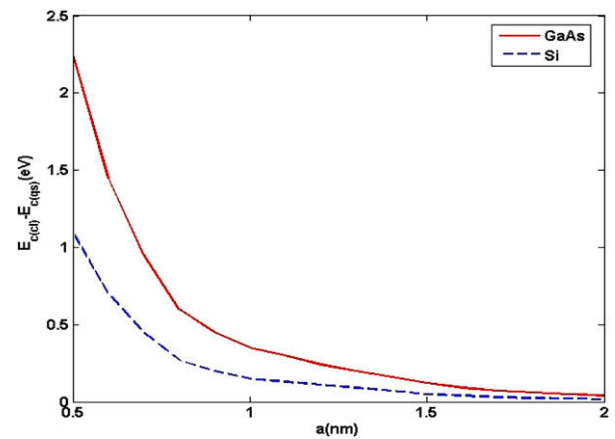


Fig. 3a. Ground state band energy shift for conduction band due to quantum confinement induced strain in a cuboidal QD.

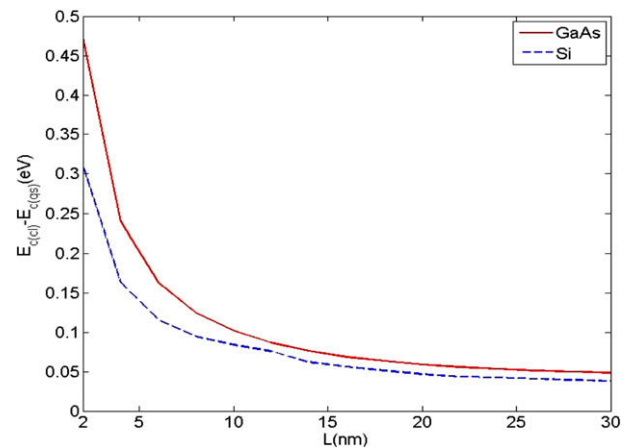


Fig. 3b. Ground state band energy shift for conduction band due to quantum confinement induced strain in a nanowire QD of cross-sectional dimension $a = 0.5$ nm and variable length L .

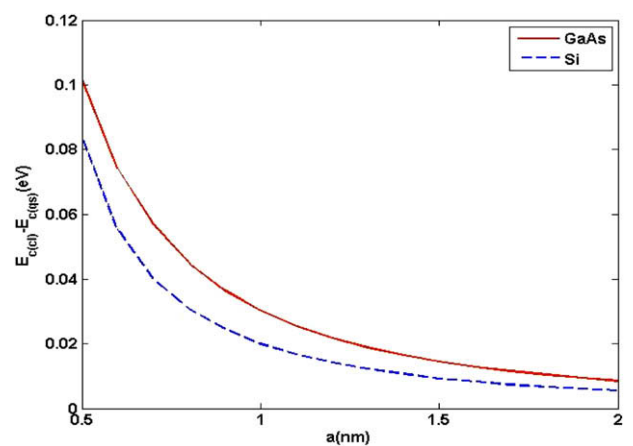


Fig. 3c. Ground state band energy shift for conduction band due to quantum confinement induced strain in a nanowire QD of length $L = 10$ nm and variable cross-sectional dimension a .

this work, we construct a long wavelength model in a manner that if quantum confinement induced strain is ignored, simplifies to the standard multi-band $\mathbf{k}\cdot\mathbf{p}$ approach. The general form of the quantum mechanical Lagrangian is:

$$L_e = \int_v \left\{ \frac{i\hbar}{2} [\Psi^\dagger \dot{\Psi} - \dot{\Psi}^\dagger \Psi] - \frac{\hbar^2}{2m} \nabla \Psi^\dagger \cdot \nabla \Psi - \Psi^\dagger \Omega(\mathbf{x}) \Psi \right\} d\mathbf{x} \quad (5)$$

$$L_i = \int_v \Psi^\dagger (-W_{\text{strain}}) \Psi d\mathbf{x}$$

where Ψ and ψ^\dagger are the spatial time dependent wave function and its Hermitian conjugate. $\Omega(\mathbf{x})$ is the external potential apart from the elastic field, while W_{strain} is the potential due the strain field. Separating the time-dependent part, $\Psi(\mathbf{x}, t) = \psi(\mathbf{x})e^{\frac{iEt}{\hbar}}$, and using the Euler-Lagrange equations, we obtain:

$$-\frac{\hbar^2}{2m} \nabla^2 \psi(\mathbf{x}) + \Omega(\mathbf{x})\psi(\mathbf{x}) + W_{\text{strain}}\psi(\mathbf{x}) = E\psi(\mathbf{x}) \quad (6)$$

$$-\nabla \cdot \left[\mathbf{C} : \boldsymbol{\varepsilon} + \underbrace{\psi(\mathbf{x})^\dagger \frac{\partial W_{\text{strain}}}{\partial \boldsymbol{\varepsilon}} \psi(\mathbf{x})}_{\boldsymbol{\varepsilon}_{\text{qs}}} \right] \quad (7)$$

With the boundary condition $[\mathbf{C} : \boldsymbol{\varepsilon} + \psi(\mathbf{x})^\dagger \frac{\partial W_{\text{strain}}}{\partial \boldsymbol{\varepsilon}} \psi(\mathbf{x})] n_j = F_i$, $\mathbf{C} : \boldsymbol{\varepsilon} + \psi(\mathbf{x})^\dagger \frac{\partial W_{\text{strain}}}{\partial \boldsymbol{\varepsilon}} \psi(\mathbf{x})$ should be equal to classical stress if boundary traction F_i is prescribed.

The strain $\boldsymbol{\varepsilon}$ can be decomposed into a classical part $\boldsymbol{\varepsilon}_{\text{cl}}$ satisfying $-\nabla \cdot [\mathbf{C} : \boldsymbol{\varepsilon}_{\text{cl}}] = 0$ and a non-classical part $\boldsymbol{\varepsilon}_{\text{qs}}$ such that

$$\boldsymbol{\varepsilon} = \boldsymbol{\varepsilon}_{\text{qs}} + \boldsymbol{\varepsilon}_{\text{cl}}$$

and

$$\boldsymbol{\varepsilon}_{\text{qs}} = -\mathbf{S} : \psi(\mathbf{x})^\dagger \frac{\partial W_{\text{strain}}}{\partial \boldsymbol{\varepsilon}} \psi(\mathbf{x}) \quad (8)$$

where \mathbf{S} is the elastic compliance tensor. Here the subscript *qs* denotes quantum confinement induced strain.

The Multi-band EFM, or the \mathbf{k}, \mathbf{p} method, is based on expanding the wave function in terms of atomic functions basis (Wang and Zunger, 1996) or

$$\psi(\mathbf{r}) = \sum_{n=1}^{N_b} \left[\sum_{\mathbf{k}} b_n(\mathbf{k}) e^{i\mathbf{k} \cdot \mathbf{r}} \right] \phi_{n, \mathbf{k}=0}(\mathbf{r}) \quad (9)$$

where The terms $\sum_{\mathbf{k}} b_n(\mathbf{k}) e^{i\mathbf{k} \cdot \mathbf{r}}$ are the envelope functions. N_b is the number of bands, and $\phi_{n, \mathbf{k}=0}(\mathbf{r})$ is the Bloch wave functions at $\mathbf{k}=0$. It is common practice to transform Eq. (6) into the EFM model given by

$$\sum_m (H_{nm}(\mathbf{r}) + W_{nm}(\mathbf{r})) F_m(\mathbf{r}) = E F_n \quad (10)$$

where $F_n = \sum_{\mathbf{k}} b_n(\mathbf{k}) e^{i\mathbf{k} \cdot \mathbf{r}}$. In a typical four band Luttinger–Bir–Pikus model (Bir and Pikus, 1974; Kane, 1966), $H_{nm}(\mathbf{r})$ and $W_{nm}(\mathbf{r})$ are defined by the matrices of differential operators given by

$$H_{mn} = \begin{bmatrix} -P + Q & -S^\dagger & R & 0 \\ -S & -P - Q & 0 & R \\ R^\dagger & 0 & -P - Q & S^\dagger \\ 0 & R^\dagger & S & -P + Q \end{bmatrix} \quad (11)$$

$$W_{mn} = \begin{bmatrix} -p + q & -s^\dagger & r & 0 \\ -s & -p - q & 0 & r \\ r^\dagger & 0 & -p - q & s^\dagger \\ 0 & r^\dagger & s & -p + q \end{bmatrix} \quad (12)$$

where,

$$P = -E_v - \gamma_1 \frac{\hbar^2}{2m} \nabla^2$$

$$Q = -\gamma_2 \frac{\hbar^2}{2m} (\partial_x^2 + \partial_y^2 - 2\partial_z^2)$$

$$R = \sqrt{3} \frac{\hbar^2}{2m} [\gamma_2 (\partial_x^2 - \partial_y^2) - 2i\gamma_3 \partial_x \partial_y]$$

$$S = \sqrt{3} \gamma_3 \frac{\hbar^2}{2m} \partial_z (\partial_x - i\partial_y) \quad (13)$$

$$p = a_v (\varepsilon_{xx} + \varepsilon_{yy} + \varepsilon_{zz})$$

$$q = b \left[\varepsilon_{zz} - \frac{1}{2} (\varepsilon_{xx} + \varepsilon_{yy}) \right]$$

$$r = \frac{\sqrt{3}}{2} b (\varepsilon_{xx} - \varepsilon_{yy}) - id\varepsilon_{xy}$$

$$s = -d(\varepsilon_{xz} + i\varepsilon_{yz})$$

The material parameters in the expressions listed above are generally evaluated empirically or through ab initio calculations and are listed in Appendix A for the materials (Si and GaAs) investigated in this work.

Eq. (8) also has to be cast into a multiband framework. The $\psi(\mathbf{r})^\dagger \frac{\partial W_{\text{strain}}}{\partial \boldsymbol{\varepsilon}_{ij}} \psi(\mathbf{r})$ expression can be rewritten as

$$\psi^\dagger D_{ij} \psi = \langle \alpha | \mathbf{x} \rangle \langle \mathbf{x} | \hat{D}_{ij} | \alpha \rangle \quad (14)$$

where $D_{ij} = \frac{\partial W_{\text{strain}}}{\partial \varepsilon_{ij}}$ is a differential operator while \hat{D}_{ij} is the corresponding quantum operator. They are related through $\langle \mathbf{x} | \hat{D}_{ij} | \mathbf{x}' \rangle = D_{ij}(\mathbf{x}') \delta(\mathbf{x} - \mathbf{x}')$. The wave function is the position operator on a specific quantum state, i.e. $\psi(\mathbf{r}) = \langle \mathbf{x} | \alpha \rangle$.

Eq. (14) may be expanded on position operator \mathbf{x}' as

$$\psi^\dagger D_{ij} \psi = \int_{\mathbf{x}'} \langle \alpha | \mathbf{x} \rangle \langle \mathbf{x} | \hat{D}_{ij} | \mathbf{x}' \rangle \langle \mathbf{x}' | \alpha \rangle \quad (15)$$

Using Eq. (9) we have

$$\begin{aligned} \psi^\dagger D_{ij} \psi &= \int_{\mathbf{x}'} \sum_{n=1}^{N_b} \left[\sum_{\mathbf{k}} b_n(\mathbf{k}) e^{i\mathbf{k} \cdot \mathbf{x}'} \right] \phi_{n, \mathbf{k}=0}^\dagger(\mathbf{x}') \langle \mathbf{x} | \hat{D}_{ij} | \mathbf{x}' \rangle \\ &\times \sum_{m=1}^{N_b} \left[\sum_{\mathbf{k}} b_m(\mathbf{k}') e^{i\mathbf{k}' \cdot \mathbf{x}'} \right] \phi_{m, \mathbf{k}=0}(\mathbf{x}') \end{aligned} \quad (16)$$

This can be further simplified to

$$\begin{aligned} \psi^\dagger D_{ij} \psi &= \sum_{m=1}^{N_b} \sum_{n=1}^{N_b} \left[\sum_{\mathbf{k}} b_n(\mathbf{k}) \int_{\mathbf{x}'} \left[\phi_{n, \mathbf{k}=0}^\dagger(\mathbf{x}') \langle \mathbf{x} | \hat{D}_{ij} | \mathbf{x}' \rangle \phi_{m, \mathbf{k}=0}(\mathbf{x}') \right. \right. \\ &\left. \left. \times e^{i(\mathbf{k}-\mathbf{k}') \cdot \mathbf{x}'} \right] d\mathbf{x}' \sum_{\mathbf{k}'} b_m(\mathbf{k}') \right] \end{aligned} \quad (17)$$

While,

$$\int_{\mathbf{x}'} \left[\phi_{n, \mathbf{k}=0}^\dagger(\mathbf{x}') \langle \mathbf{x} | \hat{D}_{ij} | \mathbf{x}' \rangle \phi_{m, \mathbf{k}=0}(\mathbf{x}') e^{i(\mathbf{k}-\mathbf{k}') \cdot \mathbf{x}'} \right] d\mathbf{x}' = D_{ij}^{nm} \delta_{\mathbf{k}, \mathbf{k}'} \quad (18)$$

here D_{ij}^{nm} are the components of D_{ij} in a Hilbert space consisting of the atomic basis m and n . Therefore we can further simplify Eq. (17) to be

$$\begin{aligned}
 \psi^\dagger D_{ij} \psi &= \sum_{m=1}^{N_b} \sum_{n=1}^{N_b} \left[\sum_k b_n(k) D_{ij}^{mn} \delta_{k,k'} \sum_{k'} b_m(k') \right] \\
 &= \sum_{m=1}^{N_b} \sum_{n=1}^{N_b} \left[\sum_k b_n(k) D_{ij}^{mn} b_m(k) \right] \\
 &= \sum_{m=1}^{N_b} \sum_{n=1}^{N_b} \left[\sum_k b_n(k) e^{-ik \cdot x} D_{ij}^{mn} b_m(k) e^{ik \cdot x} \right] \\
 &= \sum_{m=1}^{N_b} \sum_{n=1}^{N_b} \left[\sum_k F_n^\dagger(\mathbf{x}) D_{ij}^{mn} F_m(\mathbf{x}) \right] \quad (19)
 \end{aligned}$$

Eq. (19) may be substituted in Eq. (8) to finally yield

$$\varepsilon_{ij} = \varepsilon_{ij}^{\text{cl}} - S_{ijkl} = \sum_{m=1}^{N_b} \sum_{n=1}^{N_b} [F_n^\dagger(\mathbf{x}) D_{kl}^{mn} F_m(\mathbf{x})] \quad (20)$$

where D_{ij}^{nm} is a new term that may be written in matrix form as

$$D_{ij}^{nm} = \begin{bmatrix} -a_\nu \delta_{ij} + q_{ij} & -s_{ij}^* & r_{ij} & 0 \\ -s_{ij} & -a_\nu \delta_{ij} - q_{ij} & 0 & r_{ij} \\ r_{ij}^* & 0 & -a_\nu \delta_{ij} - q_{ij} & s_{ij}^* \\ 0 & r_{ij}^* & s_{ij} & -a_\nu \delta_{ij} + q_{ij} \end{bmatrix} \quad (21)$$

with

$$q_{ij} = \begin{bmatrix} -\frac{b}{2} & 0 & 0 \\ 0 & -\frac{b}{2} & 0 \\ 0 & 0 & b \end{bmatrix} \quad r_{ij} = \begin{bmatrix} \frac{\sqrt{3}b}{2} & -id & 0 \\ -id & -\frac{\sqrt{3}b}{2} & 0 \\ 0 & 0 & 0 \end{bmatrix} \quad s_{ij} = \begin{bmatrix} 0 & 0 & -d \\ 0 & 0 & id \\ -d & id & 0 \end{bmatrix} \quad (22)$$

This completes the development of the multiband $\mathbf{k} \cdot \mathbf{p}$ method. We now formulate expressions for various energy terms.

The total ground state energy of the system is

$$\begin{aligned}
 E_{\text{tot}} &= \int_V [F_n^\dagger(\mathbf{x}) H_{nm}(\mathbf{x}) F_m(\mathbf{x})] d\mathbf{x} + \int_V [F_n^\dagger(\mathbf{x}) D_{ij}^{nm} \varepsilon_{ij} F_m(\mathbf{x})] d\mathbf{x} \\
 &\quad + \frac{1}{2} \int_V \sigma_{ij} \varepsilon_{ij} d\mathbf{x} \quad (23)
 \end{aligned}$$

The normalization constrain is $\int_V F_n^\dagger(\mathbf{x}) F_n(\mathbf{x}) d\mathbf{x} = 1$, Einstein summation notation is not adopted here. The envelope function $F_m(\mathbf{x})$ and the strain ε_{ij} minimize the total energy E_{tot} . If we consider ΔE as the shift of the ground energy, incorporating this reverse coupling, the relative polaron binding energy is defined as $-\Delta E$ (Alexandre et al., 2003). Where,

$$\Delta E = \int_V [F_n^\dagger(\mathbf{x}) D_{ij}^{nm} \varepsilon_{ij} F_m(\mathbf{x})] d\mathbf{x} + \frac{1}{2} \int_V \sigma_{ij} \varepsilon_{ij} d\mathbf{x} \quad (24)$$

Here, the first integral is the band energy shift due to quantum confinement induced strain and the second integral is the corresponding elastic deformation energy. Assuming no external stress is applied and assuming the absence of any pre-existing strain, from Eq. (20), the developed strain field may be written as $\varepsilon_{ij} = -S_{ijkl} F_n^\dagger(\mathbf{x}) D_{kl}^{nm} F_m(\mathbf{x})$. With the subscripts *band* and *elastic* indicating the shift of the band energy and the elastic energy, respectively, we then have:

$$\begin{aligned}
 \Delta E &= \Delta E_{\text{band}} + \Delta E_{\text{elastic}} \\
 \Delta E_{\text{band}} &= -S_{ijkl} [F_s^\dagger(\mathbf{x}) D_{ij}^{st} F_t(\mathbf{x})] [F_n^\dagger(\mathbf{x}) D_{kl}^{nm} F_m(\mathbf{x})] d\mathbf{x} \\
 \Delta E_{\text{elastic}} &= \frac{1}{2} S_{ijkl} \int_V [F_s^\dagger(\mathbf{x}) D_{ij}^{st} F_t(\mathbf{x})] [F_n^\dagger(\mathbf{x}) D_{kl}^{nm} F_m(\mathbf{x})] d\mathbf{x} \quad (25)
 \end{aligned}$$

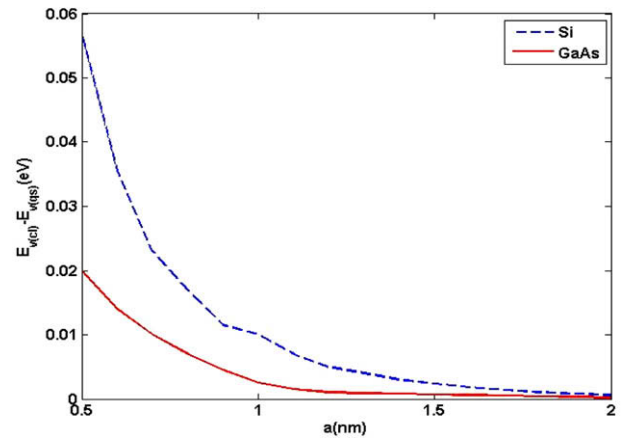


Fig. 4a. Ground state band energy shift for valence band due to quantum confinement induced strain in a cuboidal QD.

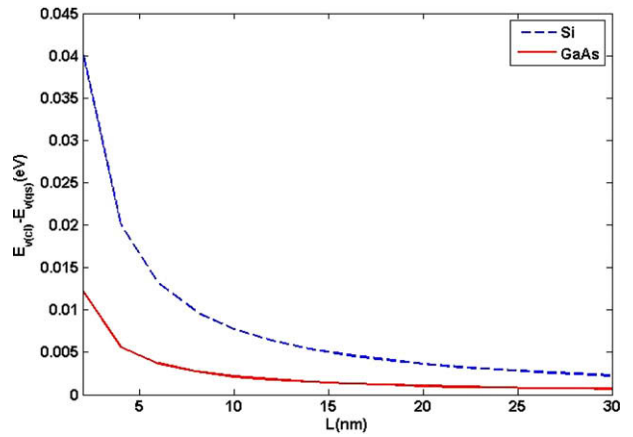


Fig. 4b. Ground state band energy shift for valence band due to quantum confinement induced strain in a nanowire QD of cross-sectional dimension $a = 0.5$ nm and variable length L .

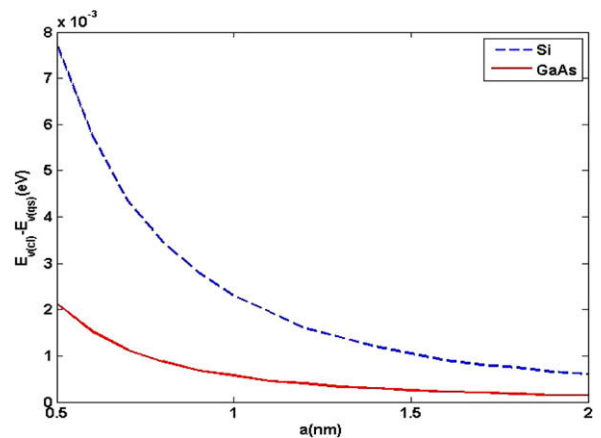


Fig. 4c. Ground state band energy shift for valence band due to quantum confinement induced strain in a nanowire QD of length $L = 10$ nm and variable cross-sectional dimension a .

This leads us to an important conclusion: $\Delta E_{\text{band}} = -2\Delta E_{\text{elast}}$. This relation is only valid for the carrier–acoustic phonon interaction and provides a simple test of the theory when we seek to confirm it using ab initio calculations.

4. Numerical results

The modified EF based model that incorporates quantum confinement induced strain developed in the preceding section is solved numerically for Si and GaAs quantum dots. Spherical, cubic and wire-shaped QDs are considered. No external stress is applied and thus $\epsilon^0 = 0$. Dirichlet boundary conditions are applied and the equations are solved in a self-consistent manner. To elaborate, the quantum confinement induced strain components in Eq. (10) are initially set to zero, which corresponds to the conventional models. Solution of the eigenvalue problem in Eq. (10) provides initial estimates of the relative envelope functions F_n for the ground state conduction or valence bands. Eq. (20) is then used to obtain modified strains that are inserted into Eq. (10) for further iteration. This self-consistent scheme is carried out until the difference between the successive ground state band energies is less than 0.0001 eV.

The system of self-consistent equations (Eqs. (4), (10) and (20)) is solved numerically using the finite difference method. An appropriate discrete scheme needs to be chosen to remove the nonhermicity of the differential in a regular center discrete scheme. Alternatively, one could develop a finite element scheme as was done for the classical EF approach by Johnson et al. (1998). We note here that spurious results can be produced if the discrete scheme is not chosen properly (e.g. Godfrey and Malik, 1996; Meney et al., 1994; Szmulowicz, 2005). In our numerical calculations of the developed EF model, a relatively well-tested discrete scheme is chosen to retain the hermicity of the differential operator (Burt, 1992, 1999). Thus,

$$A \frac{\partial}{\partial x_i} \Rightarrow \frac{1}{2} \left(A \frac{\partial}{\partial x_i} + \frac{\partial}{\partial x_i} A \right)$$

$$A \frac{\partial}{\partial x_i} \frac{\partial}{\partial x_j} \Rightarrow \frac{1}{2} \left(\frac{\partial}{\partial x_j} A \frac{\partial}{\partial x_i} + \frac{\partial}{\partial x_i} A \frac{\partial}{\partial x_j} \right)$$
(26)

The first and second derivatives are therefore discretized using this central difference scheme for position dependent variable A . For example, the two differential operators (Eq. (26)) are written in discrete form along the x -direction as

$$A \frac{\partial}{\partial x} F \Big|_{x=x_0} = \frac{[A(x_0+d)+A(x_0)]F(x_0+d) - [A(x_0-d)+A(x_0)]F(x_0-d)}{4d}$$

$$A \frac{\partial^2}{\partial x^2} F \Big|_{x=x_0} = \frac{[A(x+d)+A(x)][F(x+d)-F(x)]}{2d^2} - \frac{[A(x)+A(x-d)][F(x)-F(x-d)]}{2d^2}$$
(27)

Here d is the finite difference step size along the x -direction.

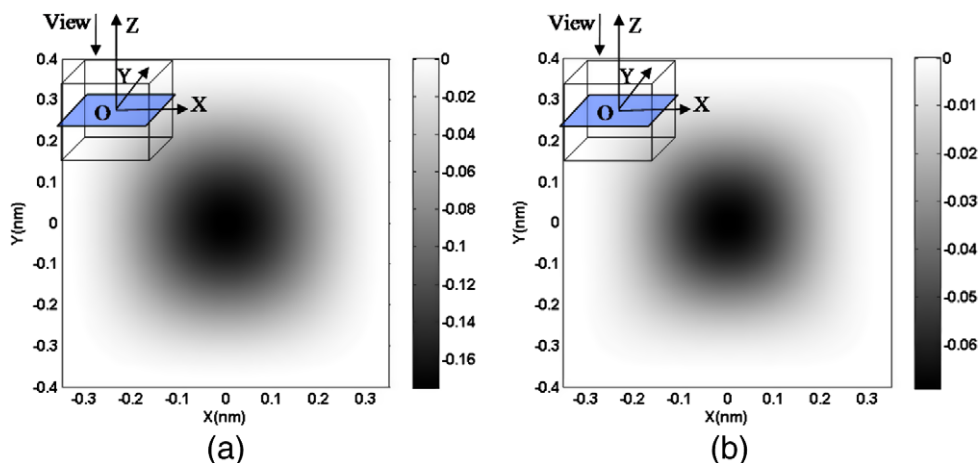


Fig. 5. Magnitude of the strain (dilation) for a cuboidal Si QD ($a = 7 \text{ \AA}$) on the $z = 0$ plane (shaded in the inset) viewed from top. (a) Conduction band. (b) Valence band. No external stress is applied and the strain depicted is entirely due to quantum confinement.

For both the single band and four band models, at each self-consistent loop, a large scale linear eigen-system is solved. The linear eigenvalue problem in each iteration is handled by the blocked Jacobi–Davidson method in shift and invert mode (Sleijpen and Van der Vorst, 1996). The conventional Jacobi pre-conditioner is used to speed up convergence. The necessary material parameters are presented in Appendix A.

The numerical results for the band energy shift ($E_{c/v(ct)} - E_{c/v(qs)}$) in the GaAs and Si quantum dots are presented in Figs. 3(a)–(c) and 4(a)–(c). Here subscripts c and v indicate conduction and valence bands, respectively.

Based on the toy model developed in Section 2, we expect $E_{c/v(ct)} - E_{c/v(qs)}$ to roughly scale with $-\frac{a^2}{K} |\psi(\mathbf{r})|^2$. This energy difference is size-dependent and quadratic in the deformation potential constant. Thus, as evident in panels (a)–(c) we expect the GaAs QD to have larger quantum confinement induced strain coupling than Si, as the conduction band deformation potential of GaAs is nearly 1.5 times that of Si. In panels (a)–(c) the silicon QD valence band energy exhibits a larger shift than GaAs due to its higher valence band deformation potential. We finally note that quantum confinement induced strain is very small for quantum dots with size larger than 2 nm emphasizing the strong role of size in this peculiar type of coupling.

The dilation due to electron and holes is plotted in Fig. 5 for a cuboidal Si quantum dot.

The dilation strain induced by the electron confinement effect is much larger than that induced by the hole due a large difference in their deformation potentials. The strain fields induced by the ground state hole are more complicated due to the multiband interactions.

For the electron induced strain (Fig. 5(a)), the only nonzero strain fields are $\epsilon_{xx} = \epsilon_{yy} = \epsilon_{zz}$. This is different from the hole induced strain field described by the four band model. The three shear strains are highly non-uniform and interestingly, the volume average of the dilation induced by the hole polarons is nearly zero. This is explained by noting that the strain contributions from the heavy hole band and the light hole band offset each other. The volume averages of shear stresses induced by valence hole are always zero, due to the orthogonality between different envelope functions.

The strain distribution in a cuboidal Si QD is shown in Fig. 6 while the size-dependency of the quantum confinement induced strain field (maximum value) is depicted in Figs. 7 and 8.

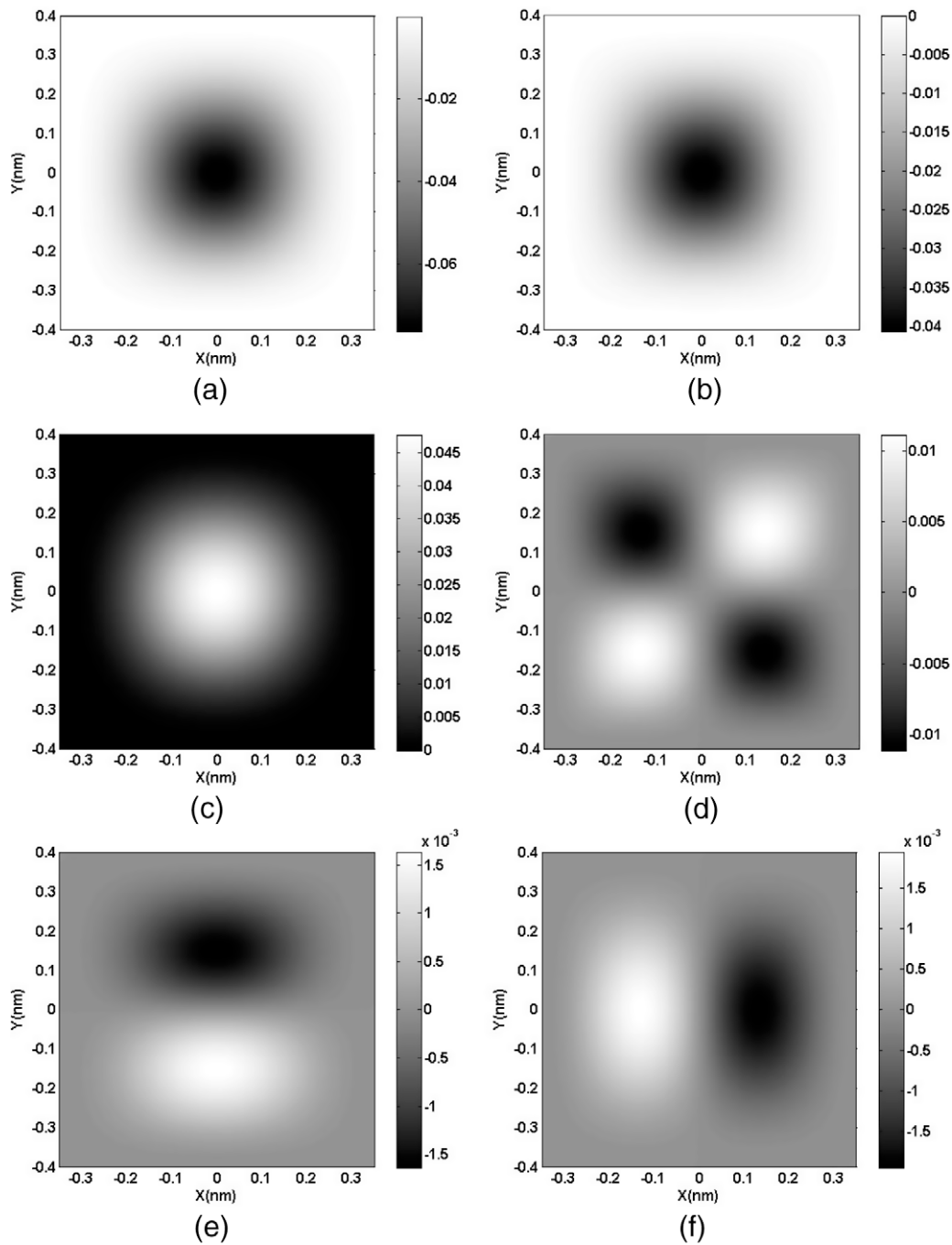


Fig. 6. Distribution of strain fields induced by a confined hole in a cuboidal Si QD ($a = 7 \text{ \AA}$) on the $z = 0$ plane. (a) ϵ_{xx} , (b) ϵ_{yy} , (c) ϵ_{zz} , (d) ϵ_{xy} , (e) ϵ_{xz} , and (f) ϵ_{yz} . No external strain is applied; the strain shown here is entirely due to quantum confinement.

5. Prospects of optical actuation in nanowires

The concept of quantum possible field induced strain mediated by acoustic polarons, in principle, provides a mechanism for “actuation at a distance”. Remote actuation has numerous applications in areas as diverse as biomedical diagnostics and defense. Remote actuation may be most easily achieved via optical stimulus. Indeed, incident light of appropriate energy will create electron–hole pairs in nanowires. As results from the preceding sections show, provided that the size of the nanowire is sufficiently small, the electron and hole pairs will create polarons thus inducing mechanical strain. As was noted in the previous section, the strain due to an electron polaron does not cancel the strain due to a hole polaron.

As an illustration, the strain distribution in a (square cross-section) GaAs nanowire ($a = 0.5$ and $L = 5$ nm) is presented in Fig. 9.

The variation of the maximum strain as a function of nanowire length is shown in Figs. 10 and 11 for both Si and GaAs. If we consider a GaAs nanowire with cross-sectional dimension $a = 2$ nm and length $L = 10$ nm, the total length change in the x -direction is about 0.0008 nm. Assuming linear superposition, allowing multiple polarons to be added linearly, we deduce that the total length change for 100 polarons is about 0.8 Å. Thus an intense enough optical absorption can easily create substantial deformations. While the assumption of linear superposition can be only be rigorously correct in the dilute limit, a recent work on many-body polaron theory achieved by Maniadis et al. (2008) indicates that the

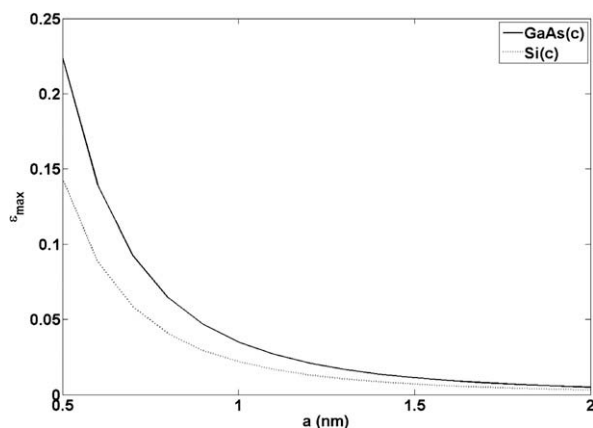


Fig. 7. Variation of the maximum strain in a cuboidal QD, $\epsilon_{\max} = \max(|\epsilon_{11}|) = \max(|\epsilon_{22}|) = \max(|\epsilon_{33}|)$.

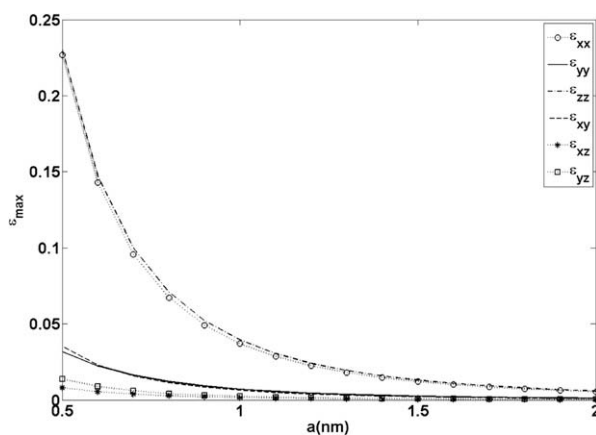


Fig. 8. Variation of the maximum strain in a cuboidal GaAs QD, where $\epsilon_{\max} = \max(|\epsilon_{ij}|)$.

energy per polaron changes by less than 0.7% corresponding to a nearly 37% change in the number of polarons. Clearly, while the interaction energy plays a role, our linear superposition based computation is at least approximately correct. Limited experimental evidence (in the context of carbon nanotubes) may be cited. A theoretical model involving polarons, based on the effective mass approximation, was suggested by Verissimo-Alves et al. (2001) to explain nanotube expansion in the experiments of Baughman et al. (1999) upon electron doping. Zhang and Iijima (1999) also observe macroscopic displacement of carbon nanotube bundles under visible light illumination. This displacement is also attributed to the formation of polarons by Verissimo-Alves et al.

6. Ab initio calculations and comparison

In this Section, we present ab initio calculations to verify our model and obtain additional insights. A straightforward way to reconcile the concept of quantum-confinement-induced-strain and polarons and to validate our modified EFM model is to contrast the computed electron polaron binding energy with ab initio calculations.

Various sized clusters for this study are constructed via truncation of a bulk crystal. The truncation is carefully performed to ensure that no single atom has less than two dangling bonds for materials with diamond like structure. The obtained nanoclusters are appropriately passivated to saturate all the dangling bonds

and keep the clusters charge neutral. The resulted neutral clusters are atomically relaxed via various schemes. This last step, while time consuming, is quite important as it *eliminates the surface relaxation induced strain effects*. After relaxation, an electron or hole is doped into the QD and relaxed further from the optimized state of the neutral QD. The change of the total energy from non-relaxed to relaxed doped quantum dot is the polaron binding energy (Alexandre et al., 2003).

The atomistic calculations are carried out by including both DFT approach and a semi-empirical method (which is more computationally expedient for larger sizes). The quantum dots with fewer than 500 atoms were performed by the DFT method. The DFT calculation was done using OpenMX² and PWSCF³ with the direct inversion iterative sub-space (DIIS) method and the quasi-Newton Broyden–Fletcher–Goldfarb–Shanno (BFGS) method, respectively, for the geometrical relaxation. The local density approximation is applied with the Ceperley–Alder functional (LDA-CA) and generalized gradient approximation of the Perdew–Burke–Ernzerhof functional (GGA-PBE) without spin-orbital coupling. The geometric relaxation criterion is chosen as 0.02 eV/Å. For larger sized quantum dots, the semi-empirical simulation is performed using PM3 geometric optimization in the GAMESS package⁴ only for silicon quantum dots. The geometric relaxation convergence criterion requires a density gradient of less than 0.005 eV/Å between two sequential relaxation steps to ensure energy tolerance of less than 0.5 meV. Unrestricted Open Shell Hartree–Fock (UHOF) self-consistent field (SCF) is chosen with the DIIS mixing to speed up the SCF calculation for carrier doped quantum dots.

There are two important issues related to the DFT calculation. The first one is the passivation of the dangling bonds of QDs. It is necessary to eliminate the surface states between the LUMO (Lowest Unoccupied Molecular Orbital) and the HOMO (Highest Occupied Molecular Orbital) in the electronic spectrum. One single valence bond must contain two electrons. For type IV semiconductors, such as Si, one unsaturated dangling bond contains one electron. Therefore, a regular hydrogen atom can be used to passivate the dangling bond. However, the valence bonds of type II–VI or III–V semiconductors are polarized and the dangling bonds contain partial charges. For example the Cd atom (of the CdSe QD) contains 0.5 valence charge. This requires a pseudo-hydrogen passivating atom, symbolized as X, with 1.5 valence charge, while maintaining the overall charge neutrality of the quantum dot. The next step is to determine the bond length of Cd–X. Typically the tetrahedral structure CdX₄ is configurationally relaxed to determine the Cd–X bond length. In our simulations, the dangling bond length of Cd–X is found to be 1.80 Å and of Se–Xa is 1.59 Å, where Xa is a neutral pseudo-hydrogen atom with 0.5 core and valence charge. Interested readers are referred to Huang et al. (2005) and references therein for further information on this passivation method.

As is well known, DFT is suitable for ground state total energy calculations underestimates energy gaps. Remedies exist to correct this (Degoli et al., 2004; Hedin, 1965; Puzder et al., 2003; Zunger, 2001). In any event, detailed calculations examining the accuracy of DFT for strain–electronic structure coupling were done (Peng et al., 2006) in which the super cell DFT results are compared with a more accurate configuration interaction singles calculation as well as an all-electron basis method calcu-

² Order N DFT code, OpenMX, available on <http://staff.aist.go.jp/t-ozaki> in the constitution of the GNU GPL.

³ PWSCF available on <http://www.pwscf.org> in the constitution of the GNU GPL.

⁴ The General Atomic and Molecular Electronic Structure System (GAMESS) is available on <http://www.msg.ameslab.gov/GAMESS/> in the constitution of the GNU GPL.

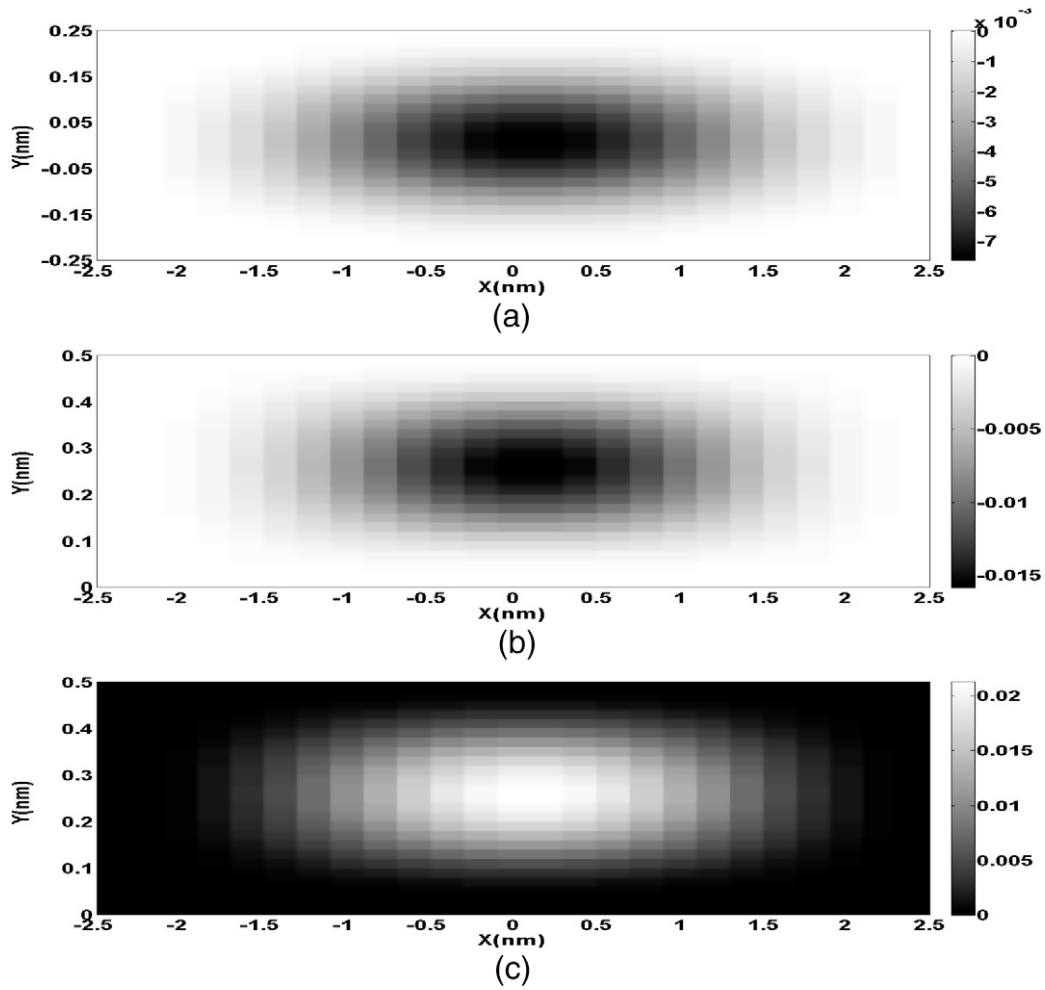


Fig. 9. Distribution of strain fields induced by a hole confined in a GaAs nanowire ($a = 0.5$ and $L = 5$ nm) on the $z = 0$ plane, (a) ϵ_{xx} , (b) ϵ_{yy} , (c) ϵ_{zz} , (d) ϵ_{xy} , (e) ϵ_{xz} , and (f) ϵ_{yz} . No external strain is applied and the strain shown here is entirely due to quantum confinement.

lation. Reasonable qualitative and quantitative agreement is found.

In Fig. 12 we compare the polaron binding energy predicted from our modified EF model, the conventional EF method (the dotted horizontal line) and our ab initio simulations for the Si quantum dots. As shown in the figure, the polaron binding energy from our model, which is half of the band energy shift, matches very well with the atomistic results. The conventional \mathbf{k}, \mathbf{p} approach breaks down for electronic structure calculations around 4 nm or higher. In contrast, the polaron binding energy is in good agreement with atomistic results down to nearly 0.6 nm

Fig. 13 is our density functional calculation result (within the LDA approximation) for silicon QDs, measured by $E_{pb} - \frac{E_{c/v}(cl) - E_{c/v}(qs)}{2}$. The results verify our theoretical conclusion in Section 3 regarding the relationship of the polaron binding energy and the band energy shift, namely, that the band energy shift should be twice the polaron binding energy, which implies that $E_{pb} - \frac{E_{c/v}(cl) - E_{c/v}(qs)}{2}$ has to be zero according to our EFM model. As far as we know this principle only holds for electron–acoustic phonon interaction. Therefore, we can also provide a rough estimation of the extent of electron–optical phonon interaction through the measurement $M = E_{pb} - \frac{E_{c/v}(cl) - E_{c/v}(qs)}{2}$. The closer M is to zero, the larger the electron–acoustic phonon interaction. In the semiconductor industry, CdSe is an important polar semiconductor materials wherein opti-

cal polarons are likely to be significant. The electron–optical phonon interaction in spherical CdSe QDs is compared with that in spherical Si QDs in Fig. 10 with the DFT (LDA) results of CdSe QDs presented in Table 1.

In Fig. 14, $E_{pb} - \frac{E_{c/v}(cl) - E_{c/v}(qs)}{2}$ is plotted for spherical Si and CdSe QDs. As evident, the electron–optical phonon interaction is important in the CdSe quantum dots as anticipated, but diminishes rapidly with increasing size. For quantum dots with size larger than 7 Å the acoustic polaronic effect appears to be dominant. As expected, since Silicon is nonpolar, the acoustic polaronic effect dominates for all sizes.

The modified EF model does not appear to describe hole polarons well (when compared with DFT calculations) as shown in Fig. 15. This discrepancy may be due to the use of the EF approach for such small sizes and perhaps more bands or a tight binding based approach may yield better accuracy. However, the main intent in developing an EF based approach is to provide analytical transparency in identifying this unusual effect.

Molecular orbital (MO) or wave function plots are shown in Fig. 16. The MOs are real valued functions in this case since spin orbital coupling is ignored. Therefore, the MOs span the same area with the isosurfaces of the particle density with the square value (0.015 or 0.02): 25% or 50% of the maximums of ground state conduction and valence MOs according to Fig. 15. The MO is for ground state conduction band of the electron doped

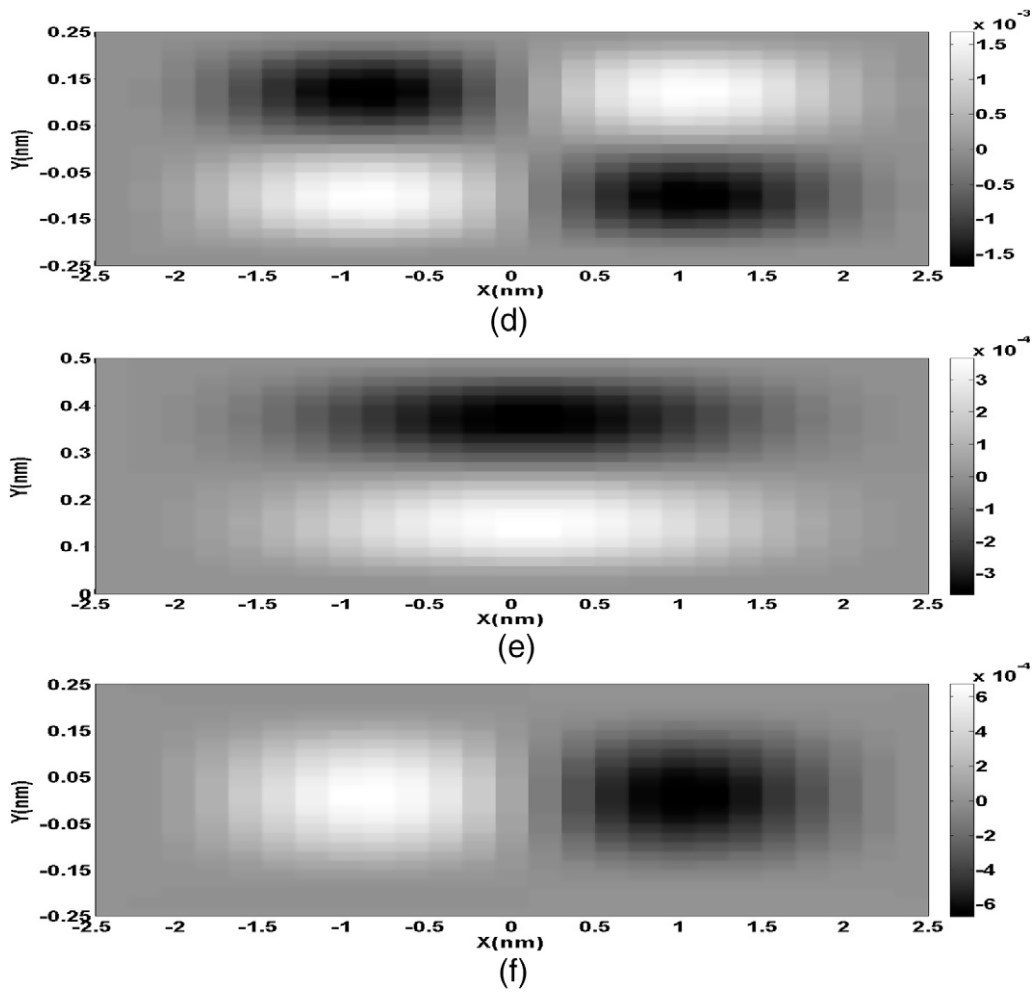


Fig. 9 (continued)

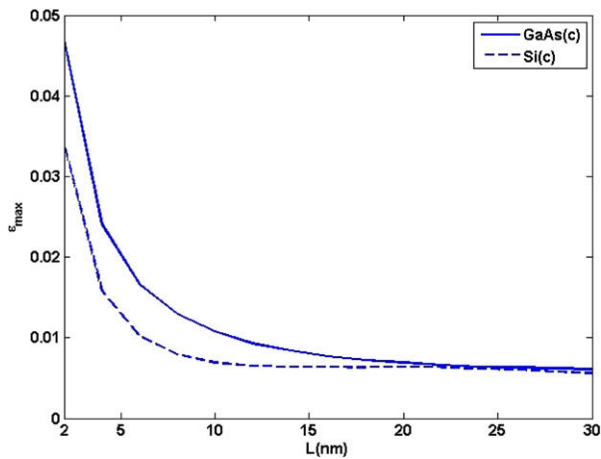


Fig. 10. Variation of the maximum strain with length L for a nanowire with cross-sectional dimension $a = 0.5$ nm and $\epsilon_{\max} = \max(|\epsilon_{11}|) = \max(|\epsilon_{22}|) = \max(|\epsilon_{33}|)$.

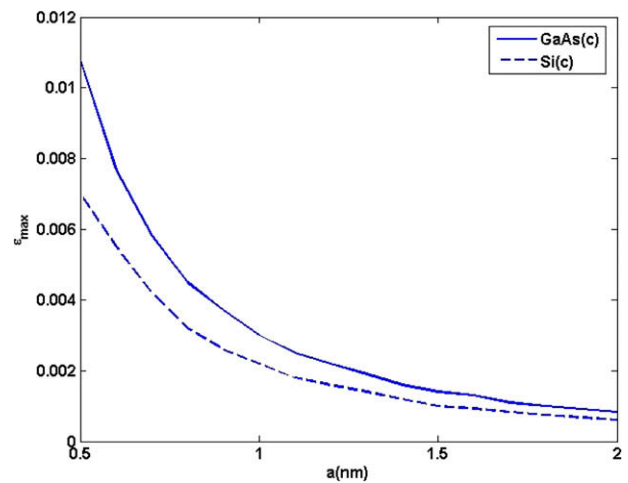


Fig. 11. Variation of the maximum strain with cross-sectional dimension a for nanowires with length $L = 10$ nm and $\epsilon_{\max} = \max(|\epsilon_{11}|) = \max(|\epsilon_{22}|) = \max(|\epsilon_{33}|)$.

QD before and after the formation of a polaron. The bonding character and anti-bonding character are still prominent for the HOMO (highest occupied molecular orbital) and LUMO (lowest unoccupied molecular orbital) in the doped quantum dot. There exists a contraction of the area spanned by $|0.015|$ isosurface and a very large ($\sim 100\%$) increase of maximum MO value between

them. This implies an increase of quantum confinement for the electron. This feature is also correctly predicted by the modified $\mathbf{k}\cdot\mathbf{p}$ model (see Fig. 17).

Fig. 17(a) shows the difference of the square modulus of the electron wave function $|\psi(\mathbf{r})|_{qs}^2 - |\psi(\mathbf{r})|_{cl}^2$ based on the modified

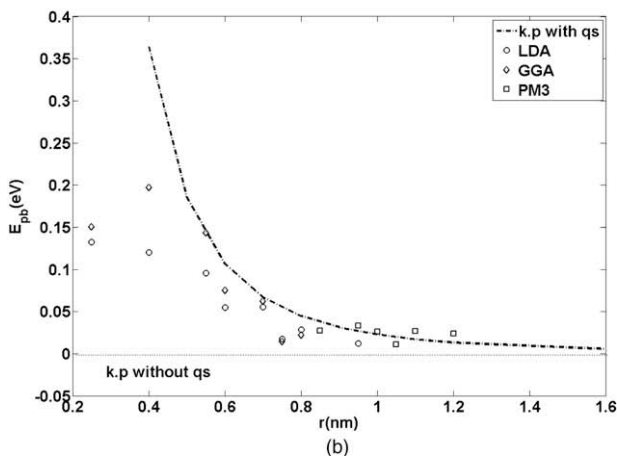
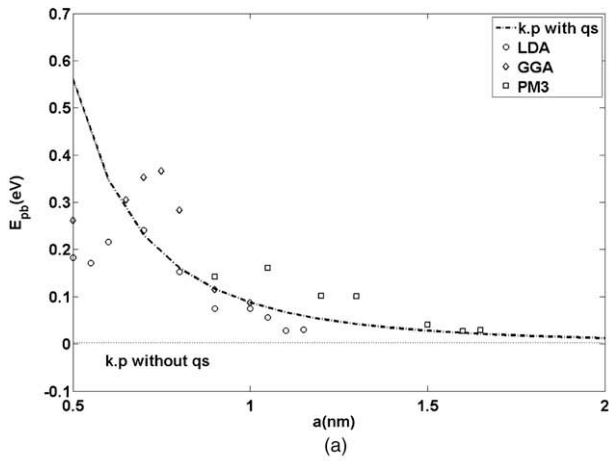


Fig. 12. Comparison of the polaron binding energy calculated from **k.p** with quantum confinement induced strain (qs in figure) and from atomistic simulations. (a) Cuboidal Si QD and (b) spherical QD.

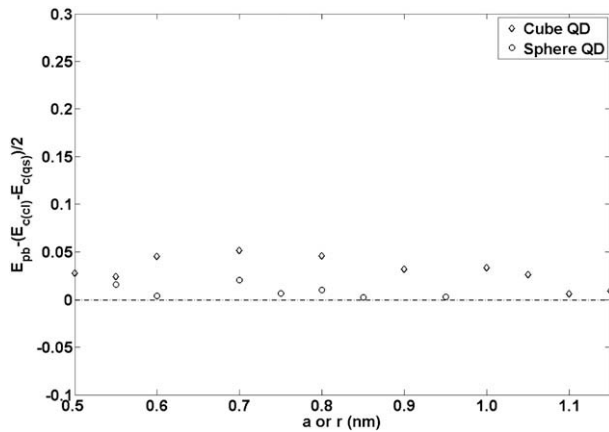


Fig. 13. The difference between electron polaron binding energy and the ground state conduction band energy shift for cuboidal and spherical silicon quantum dots, computed using DFT (LDA).

k.p model. This difference implies enhanced quantum confinement after polaron formation in the conduction band and negligible qualitative change in the valence band. As already discussed, both features are also evident in the HOMO–LUMO plots in Fig. 16.

Table 1

DFT (LDA) results for CdSe QDs. The subscript “tot” indicates the total energy. The subscript “v” indicates ground state valence hole. “–” and “+” in the brackets imply the QDs are electron or hole doped. Ry is, the atomic unit, 13.6 eV.

Radius of QD (Å)	4	5	7
$E_{\text{tot-cl}}(-)$ (Ry)	-797.148	-1663.93	-5027.67
$E_{\text{tot-qs}}(-)$ (Ry)	-797.165	-1663.95	-5027.68
$E_{\text{tot-cl}}(+)$ (Ry)	-71.0104	-1663.16	-5027.04
$E_{\text{tot-cl}}(+)$ (Ry)	-71.0194	-1663.18	-5027.05
$E_{\text{pb}}(-)$ (eV)	0.232808	0.330112	0.058492
$E_{\text{pb}}(+)$ (eV)	0.123142	0.258817	0.051179
$E_{\text{c-cl}}(-)$ (eV)	-0.6768	-1.5995	-2.1914
$E_{\text{c-qs}}(-)$ (eV)	-1.0069	-2.1982	-2.297
$E_{\text{v-cl}}(+)$ (eV)	-9.4308	-9.0874	-6.5455
$E_{\text{v-qs}}(+)$ (eV)	-9.024	-8.5715	-6.4507

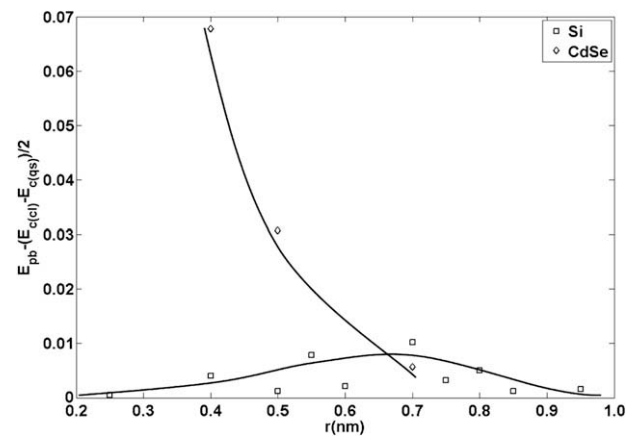


Fig. 14. Electron–optical phonon interaction for spherical Si and CdSe QDs (solid lines are guide to the eye).

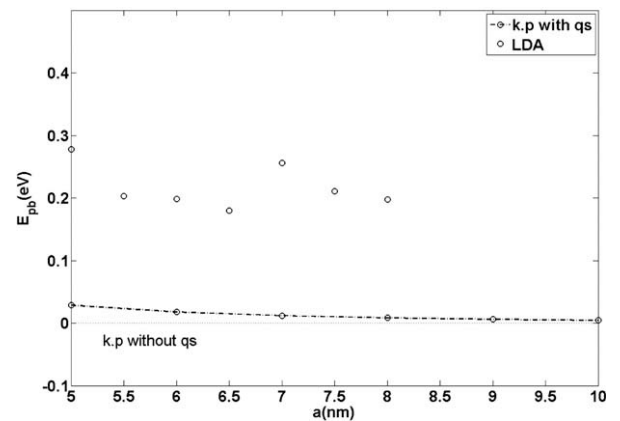


Fig. 15. Comparison of the hole polaron binding energy calculated from **k.p** with quantum confinement induced strain (qs in figure) and from atomistic simulations for cuboidal Si QDs.

7. Closure

In this paper, we explore a novel type of coupling between solid mechanics and quantum mechanics – mechanical strain induced due to changes in the quantum fields. One of the key features of this phenomenon is its *universality*. Unlike electro–mechanical coupling, the present effect in principle applies to all materials

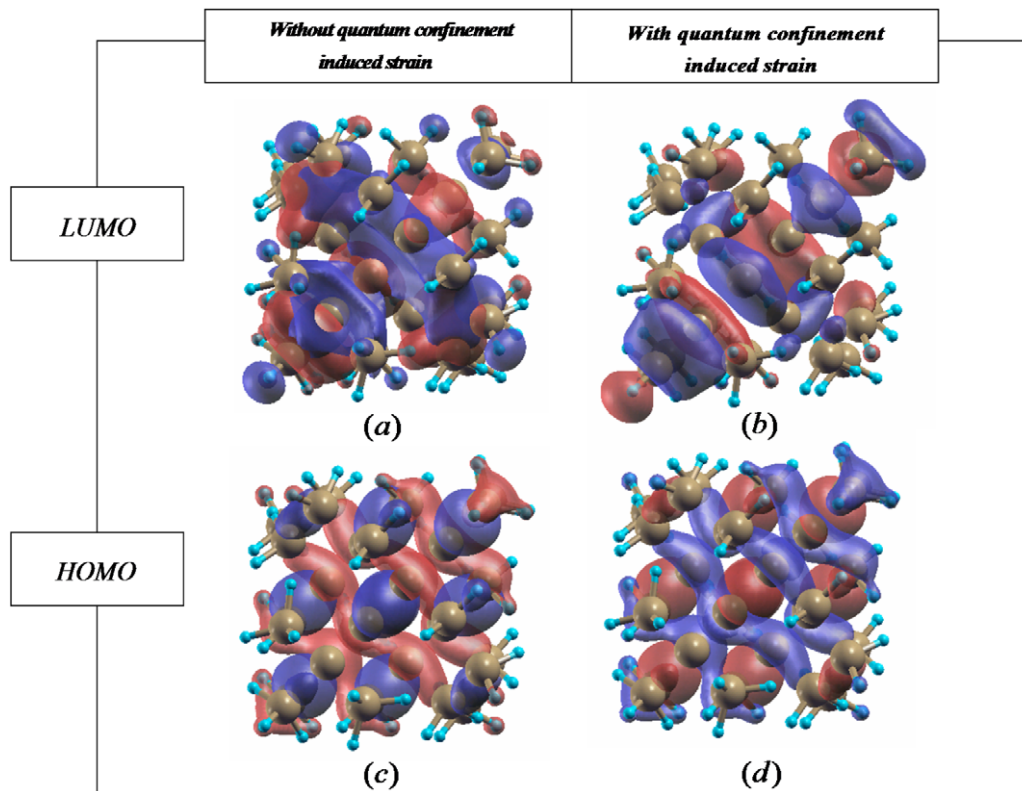


Fig. 16. Isosurface plot for the molecular orbitals (wave function) of $a = 7 \text{ \AA}$ cuboidal QD, showing both LUMO (lowest unoccupied molecules orbital) and HOMO (highest occupied molecules orbital). Red stands for positive value isosurface and blue stands for negative value isosurface. (a) The electron doped LUMO at the value of $|0.015|$ without polaron formation. (b) The electron doped LUMO at the value of $|0.015|$ with polaron formation. (c) The hole doped HOMO at the value of $|0.02|$ without polaron formation. (d) The hole doped HOMO at the value of $|0.02|$ with polaron formation. (For interpretation of the references to color in this figure legend, the reader is referred to the web version of this paper.)

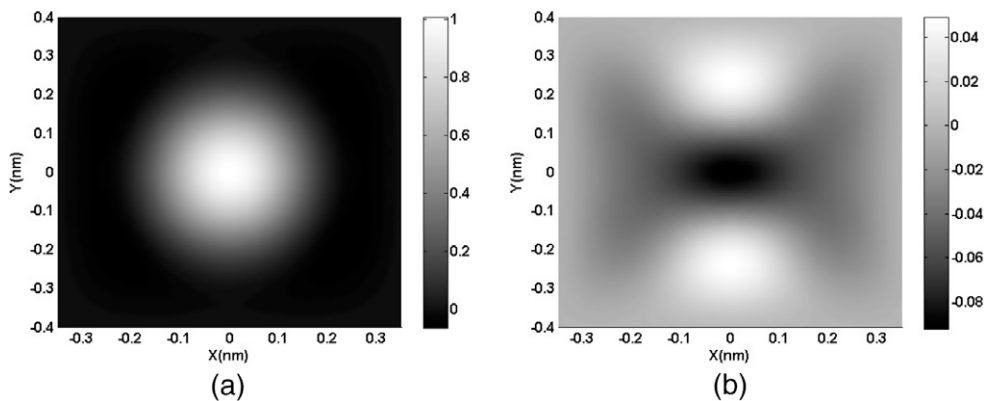


Fig. 17. Results from EFM incorporating the quantum confinement induced strain. The difference of the square modulus of the wave function (in units of nm^{-3}) without and with the formation of polaron for $a = 7 \text{ \AA}$ cubic QD for (a) electron doped ground state conduction band and (b) hole doped ground state valence band.

although it is significant only for very small sizes. While this effect is always implicitly present in *ab initio* numerical computations, our theoretical work provides an identification of the effect. We physically interpret this phenomenon in terms of the well-known theory of polarons. With appropriate engineering, the present phenomenon may provide a mechanism for optical ‘actuation-at-a-distance’ for nanowires. While only anecdotal at best, some experimental evidence also exists for this effect in the context of carbon nanotubes (CNT). A theoretical model involving polarons based on the effective mass approximation was suggested (Verissimo-Alves et al., 2001) to explain CNT expansion in the experiments of Baughman et al. (1999) upon electron doping. Zhang and Iijima (1999) observe macroscopic displacement of carbon nanotube

bundles under visible light illumination. This displacement is also attributed to the formation of polarons. We hope that the present work provides a basis for what some researchers may term quantum electro-mechanical systems.

Acknowledgments

P.S., X.Z. and M.G. acknowledge support of the ONR Young Investigator Program award-N000140510662 (Program Manager: Martin Kruger). We appreciate the discussion with Xihong Peng, Kun Jiao and Dr. Ozaki regarding the atomistic simulations. The computational facilities were provided by TLC² in University of Houston which is gratefully acknowledged.

Appendix A. Table of band structure parameters (Paul, 2004).

	GaAs	Si
m_c^{eff}	0.067	0.26
E_c (eV)	1.518	1.155
E_v (eV)	0	0
a_c (eV)	-8.013	6.4
a_v (eV)	-0.22	2.46
γ_1	7.1	4.285
γ_2	2.02	0.339
γ_3	2.93	1.446
b (eV)	-1.824	-2.33
d (eV)	-5.062	-5.32
C_{11} (GPa)	119.0	166.0
C_{12} (GPa)	53.4	64.0
C_{44} (GPa)	59.6	79.6

References

- Alexandre, S.S., Artacho, E., Soler, J.M., Chacham, H., 2003. Small polarons in dry DNA. *Physical Review Letters* 91 (10), 108105.
- Alivisatos, P., 2000. Semiconductor nanocrystals: from scaling laws to biological applications. In: *Quantum Electronics and Laser Science Conference, 2000 (QELS 2000)*, Technical Digest, p. 86.
- Andreev, A.D., Downes, J.R., Faux, D.A., O'Reilly, E.P., 1999. Strain distributions in quantum dots of arbitrary shape. *Journal of Applied Physics* 86 (1), 297–305.
- Arakawa, Y., 2002. Progress in GaN-based quantum dots for optoelectronics applications. *Selected Topics in Quantum Electronics IEEE Journal* 8 (4), 823–832.
- Bandhyopadhyay, S., Nalwa, H.S., 2003. *Quantum Dots and Nano-Wires*. American Scientific Publishers, California.
- Bastard, G., 1991. *Wave Mechanics Applied to Semiconductor Heterostructures*. Wiley, Chichester.
- Bastard, G., Verzele, O., Ferreira, R., Inoshita, T., Sakaki, H., 2002. Polaron effects in quantum dots. *Physica Status Solidi (A): Applied Research* 190 (1), 213–219.
- Baughman, R.H., Cui, C., Zakhidov, A.A., Iqbal, Z., Barisci, J.N., Spinks, G.M., Wallace, G.G., Mazzoldi, A., De Rossi, D., Rinzler, A.G., Jaschinski, O., Roth, S., Kertesz, M., 1999. Carbon nanotube actuators. *Science* 284 (5418), 1340–1344.
- Bellaiche, L., Wei, S.H., Zunger, A., 1996. Localization and percolation in semiconductor alloys: GaAsN vs GaAsP. *Physical Review B* 54 (24), 17568.
- Bernard, J.E., Zunger, A., 1994. Is there an elastic anomaly for a (001) monolayer of InAs embedded in GaAs? *Applied Physics Letters* 65 (2), 165–167.
- Bhattacharya, P., 2000. Quantum well and quantum dot lasers: from strained-layer and self-organized epitaxy to high-performance devices. *Optical and Quantum Electronics* 32 (3), 211–225.
- Bhattacharya, P., Stiff-Roberts, A.D., Krishna, S., Kennerly, S., 2002. Quantum dot infrared detectors and sources. *International Journal of High Speed Electronics and Systems* 12 (4), 969–994.
- Bimberg, D., 1999. Quantum dots: paradigm changes in semiconductor physics. *Semiconductors* 33 (9), 951–955.
- Bimberg, D., Grundmann, M., Lendenstov, N.N., 1996. *Quantum Dot Heterostructures*. Wiley, New York.
- Bir, G.L., Pikus, G.E., 1974. *Symmetry and Strain Induced Effects in Semiconductors*. Wiley, New York.
- Burt, M.G., 1992. The justification for applying the effective-mass approximation to microstructures. *Journal of Physics: Condensed Matter* 4 (32), 6651–6690.
- Burt, M.G., 1999. Fundamentals of envelope function theory for electronic states and photonic modes in nanostructures. *Journal of Physics: Condensed Matter* 11 (9), 53–83.
- Carlo, A.D., 2003. Microscopic theory of nanostructured semiconductor devices: beyond the envelope-function approximation. *Semiconductor Science and Technology* 18 (1), R1–R31.
- Chye, Y., White, M.E., Johnston-Halperin, E., Gerardot, B.D., Awschalom, D.D., Petroff, P.M., 2002. Spin injection from (Ga,Mn)As into InAs quantum dots. *Physical Review B* 66 (20), 201301.
- Cusack, M.A., Bridson, P.R., Jaros, M., 1996. Electronic structure of InAs/GaAs self-assembled quantum dots. *Physical Review B* 54 (4), R2300.
- Davies, J.H., 2000. *The Physics of Low-Dimensional Semiconductors: An Introduction*. Cambridge University Press, Cambridge.
- Davies, J.H., Bruls, D.M., Vugs, J.W.A.M., Koenraad, P.M., 2002. Relaxation of a strained quantum well at a cleaved surface. *Journal of Applied Physics* 91 (7), 4171–4176.
- Degoli, E., Cantele, G., Luppi, E., Magri, R., Ninno, D., Bisi, O., Ossicini, S., 2004. Ab initio structural and electronic properties of hydrogenated silicon nanoclusters in the ground and excited state. *Physical Review B* 69 (15), 155410–155411.
- Deppe, D.G., Huffaker, D.L., 2000. Quantum dimensionality, entropy, and the modulation response of quantum dot lasers. *Applied Physics Letters* 77 (21), 3325–3327.
- Downes, J.R., Faux, D.A., O'Reilly, E.P., 1997. A simple method for calculating strain distributions in quantum dot structures. *Journal of Applied Physics* 81 (10), 6700–6702.
- Efros, A.L., Rosen, M., 1998. Quantum size level structure of narrow-gap semiconductor nanocrystals: effect of band coupling. *Physical Review B* 58 (11), 7120.
- Ellaway, S.W., Faux, D.A., 2002. Effective elastic stiffnesses of InAs under uniform strain. *Journal of Applied Physics* 92 (6), 3027–3033.
- Emin, D., 1972. Energy spectrum of an electron in a periodic deformable lattice. *Physical Review Letters* 28 (10), 604.
- Emin, D., Holstein, T., 1976. Adiabatic theory of an electron in a deformable continuum. *Physical Review Letters* 36 (6), 323.
- Freund, L.B., Johnson, H.T., 2001. Influence of strain on functional characteristics of nanoelectronic devices. *Journal of the Mechanics and Physics of Solids* 49 (9), 1925–1935.
- Gashimzade, F.M., Babaev, A.M., Bagirov, M.A., 2000. Energy spectra of narrow- and zero-gap-semiconductor quantum dots. *Journal of Physics: Condensed Matter* 12 (36), 7923–7932.
- Glas, F., 2001. Elastic relaxation of truncated pyramidal quantum dots and quantum wires in a half space: an analytical calculation. *Journal of Applied Physics* 90 (7), 3232–3241.
- Godfrey, M.J., Malik, A.M., 1996. Boundary conditions and spurious solutions in envelope-function theory. *Physical Review B* 53 (24), 16504–16509.
- Grundmann, M., Stier, O., Bimberg, D., 1995. InAs/GaAs pyramidal quantum dots: strain distribution optical phonons and electronic structure. *Physical Review B* 52 (16), 11969.
- Hedin, L., 1965. New method for calculating the one-particle Green's function with application to the electron-gas problem. *Physical Review* 139 (3A), A796.
- Huang, X., Lindgren, E., Chelikowsky, J.R., 2005. Surface passivation method for semiconductor nanostructures. *Physical Review B* 71 (16), 165326–165328.
- Jiang, H., Singh, J., 1997. Strain distribution and electronic spectra of InAs/GaAs self-assembled dots: an eight-band study. *Physical Review B* 56 (8), 4696.
- Johnson, H.T., Bose, R., 2003. Nanoindentation effect on the optical properties of self-assembled quantum dots. *Journal of the Mechanics and Physics of Solids* 51, 2085–2104.
- Johnson, H.T., Freund, L.B., 2001. The influence of strain on confined electronic states in semiconductor quantum structures. *International Journal of Solids and Structures* 38 (6–7), 1045–1062.
- Johnson, H.T., Freund, L.B., Akyuz, C.D., Zaslavsky, A., 1998. Finite element analysis of strain effects on electronic and transport properties in quantum dots and wires. *Journal of Applied Physics* 84 (7), 3714–3725.
- Kane, E.O., 1966. *Physics of III–V compounds*. In: Willardson, R.K., Beer, A.C. (Eds.), *Semiconductors and Semimetals*. Academic Press, New York.
- Keating, P.N., 1966. Effect of invariance requirements on the elastic strain energy of crystals with application to the diamond structure. *Physical Review* 145 (2), 637.
- Korkusinski, M., Hawrylak, P., 2001. Electronic structure of vertically stacked self-assembled quantum disks. *Physical Review B* 63 (19), 195311.
- Lundstrom, T., Schoenfeld, W., Lee, H., Petroff, P.M., 1999. Exciton storage in semiconductor self-assembled quantum dots. *Science* 286 (5448), 2312–2314.
- Mahan, G.D., 2000. *Many-Particle Physics*. Kluwer Academic Plenum Publisher, New York.
- Makeev, M.A., Madhukar, A., 2003. Stress and strain fields from an array of spherical inclusions in semi-infinite elastic media: Ge nano-inclusions in Si. *Physical Review B* 67 (7), 073201.
- Maniadi, P., Lookman, T., Bishop, A.R., 2008. Elasticity driven self-organization of polarons. *Physical Review B* 78, 134304.
- Maranganti, R., Sharma, P., 2006. A review of strain field calculations in embedded quantum dots and wires. In: Reith, M., Schommers, W. (Eds.), *Handbook of Theoretical and Computational Nanotechnology*. Forschungszentrum Karlsruhe, Germany.
- Martin, R.M., 1970. Elastic properties of ZnS structure semiconductors. *Physical Review B* 1 (10), 4005.
- Meney, A.T., Gonul, B., O'Reilly, E.P., 1994. Evaluation of various approximations used in the envelope-function method. *Physical Review B* 50 (15), 10893–10904.
- Migliorato, M.A., Cullis, A.G., Fearn, M., Jefferson, J.H., 2002. Atomistic simulation of strain relaxation in $\text{In}_x\text{Ga}_{1-x}\text{As}$ /GaAs quantum dots with nonuniform composition. *Physical Review B* 65 (11), 115316.
- Minnaert, A., 2001. *Strain Aligned Excitons in Quantum Dots: Fröhlich Interaction*. Department of Physics, Eindhoven University of Technology, Eindhoven. p. 141.
- Nakamura, S., Pearton, S., Fasol, S., 2002. *The Blue Laser Diode: The Complete Story*. Springer, Berlin.
- Nishi, K., Yamaguchi, A.A., Ahopelto, J., Usui, A., Sakaki, H., 1994. Analyses of localized confinement potential in semiconductor strained wires and dots buried in lattice-mismatched materials. *Journal of Applied Physics* 76 (11), 7437–7445.
- Pan, E., Yang, B., 2001. Elastostatic fields in an anisotropic substrate due to a buried quantum dot. *Journal of Applied Physics* 90 (12), 6190.
- Paul, D.J., 2004. Si/SiGe heterostructures: from material and physics to devices and circuits. *Semiconductor Science and Technology* 19 (10), R75–R108.
- Pearson, G.S., Faux, D.A., 2000. Analytical solutions for strain in pyramidal quantum dots. *Journal of Applied Physics* 88 (2), 730–736.
- Peng, X.H., Ganti, S., Alizadeh, A., Sharma, P., Kumar, S.K., Nayak, S.K., 2006. Strain-engineered photoluminescence of silicon nanoclusters. *Physical Review B* 74 (3), 035335–035339.

- Petroff, M.P., 2003. Epitaxial growth and electronic structure of self-assembled quantum dots (in single quantum dots). *Topics in Applied Physics* 90, 1–24.
- Pollak, F.H., 1990. Effects of homogeneous strain on the electronic and vibrational levels in semiconductors. In: Pearsall, T. (Ed.), *Semiconductors and Semimetals*. Academic Science, Boston, p. 17.
- Pryor, C., 1998. Eight-band calculations of strained InAs/GaAs quantum dots compared with one-, four-, and six-band approximations. *Physical Review B* 57 (12), 7190.
- Pryor, C., Pistol, M.E., Samuelson, L., 1997. Electronic structure of strained InP/Ga_{0.51}In_{0.49}P quantum dots. *Physical Review B* 56 (16), 10404.
- Pryor, C., Kim, J., Wang, L.W., Williamson, A.J., Zunger, A., 1998. Comparison of two methods for describing the strain profiles in quantum dots. *Journal of Applied Physics* 83 (5), 2548–2554.
- Puzder, A., Williamson, A.J., Grossman, J.C., Galli, G., 2003. Computational studies of the optical emission of silicon nanocrystals. *Journal of the American Chemical Society* 125 (9), 2786–2791.
- Romanov, A.E., Beltz, G.E., Fischer, W.T., Petroff, P.M., Speck, J.S., 2001. Elastic fields of quantum dots in subsurface layers. *Journal of Applied Physics* 89 (8), 4523–4531.
- Sercel, P.C., Vahala, K.J., 1990. Analytical formalism for determining quantum-wire and quantum-dot band structure in the multiband envelope-function approximation. *Physical Review B* 42 (6), 3690.
- Sercel, P.C., Efros, A.L., Rosen, M., 1999. Intrinsic gap states in semiconductor nanocrystals. *Physical Review Letters* 83 (12), 2394.
- Shin, H., Lee, W., Yoo, Y.-H., 2003. Comparison of strain fields in truncated and untruncated quantum dots in stacked InAs/GaAs nanostructures with varying stacking periods. *Journal of Physics Condensed Matter* 15 (22), 3689–3699.
- Singh, J., 1992. *Physics of Semiconductors and Their Heterostructures*. McGraw-Hill Higher Education, New York.
- Sleijpen, G.L.G., Van der Vorst, H.A., 1996. A Jacobi–Davidson iteration method for linear eigenvalue problems. *SIAM Journal on Matrix Analysis and Applications* 17 (2), 401–425.
- Stier, O., Grundmann, M., Bimberg, D., 1999. Electronic and optical properties of strained quantum dots modeled by 8-band $k\cdot p$ theory. *Physical Review B* 59 (8), 5688.
- Stillinger, F.H., Weber, T.A., 1985. Computer simulation of local order in condensed phases of silicon. *Physical Review B* 31 (8), 5262.
- Szmulowicz, F., 2005. Solution to spurious bands and spurious real solutions in the envelope-function approximation. *Physical Review B* 71 (24), 245111–245117.
- Tadic, M., Peeters, F.M., Janssens, K.L., Korkusinski, M., Hawrylak, P., 2002. Strain and band edges in single and coupled cylindrical InAs/GaAs and InP/InGaP self-assembled quantum dots. *Journal of Applied Physics* 92 (10), 5819–5829.
- Tersoff, J., Teichert, C., Lagally, M.G., 1996. Self-organization in growth of quantum dot superlattices. *Physical Review Letters* 76 (10), 1675–1678.
- Verissimo-Alves, M., Capaz, R.B., Koiller, B., Artacho, E., Chacham, H., 2001. Polarons in carbon nanotubes. *Physical Review Letters* 86 (15), 3372.
- Wang, L.-W., Zunger, A., 1996. Pseudopotential-based multiband $k\cdot p$ method for ~250,000-atom nanostructure systems. *Physical Review B* 54 (16), 11417.
- Wang, L.-W., Zunger, A., 1999. Linear combination of bulk bands method for large-scale electronic structure calculations on strained nanostructures. *Physical Review B* 59 (24), 15806.
- Williamson, A.J., Zunger, A., 1998. Effect of interfacial states on the binding energies of electrons and holes in InAs/GaAs quantum dots. *Physical Review B* 58 (11), 6724.
- Yang, M., Sturm, J.C., Prevost, J., 1997. Calculation of band alignments and quantum confinement effects in zero- and one-dimensional pseudomorphic structures. *Physical Review B* 56 (4), 1973.
- Yu, P.Y., Cardona, M., 2004. *Fundamentals of Semiconductors: Physics and Materials Properties (Advanced Text in Physics)*. Springer, New York.
- Yu, W., Madhukar, A., 1997a. Molecular dynamics study of coherent island energetics, stresses, and strains in highly strained epitaxy. *Physical Review Letters* 79 (5), 905.
- Yu, W., Madhukar, A., 1997b. Molecular dynamics study of coherent island energetics, stresses, and strains in highly strained epitaxy [Phys. Rev. Lett. 79 (1997) 905]. *Physical Review Letters* 79 (24), 4939.
- Zhang, Y., 1994. Motion of electrons in semiconductors under inhomogeneous strain with application to laterally confined quantum wells. *Physical Review B* 49 (20), 14352.
- Zhang, Y., Iijima, S., 1999. Elastic response of carbon nanotube bundles to visible light. *Physical Review Letters* 82 (17), 3472.
- Zhang, X., Sharma, P., Johnson, H.T., 2007. Quantum confinement induced strain in quantum dots. *Physical Review B* 75 (15), 155318–155319.
- Zunger, A., 2001. Pseudopotential theory of semiconductor quantum dots. *Physica Status Solidi B* 224, 727–734.